Journal of ELECTRONIC MATERIALS, Vol. 41, No. 1, 2012
DOI: 10.1007/s11664-011-1757-z

Thermodynamic Description of the Quaternary Ag-Cu-In-Sn System

WOJCIECH GIERLOTKA[1,2]

1.—Chemical Engineering and Material Science Department, Yuan-Ze University, Yuan-tung Rd. 135, Chungli, Taiwan. 2.—e-mail: wojtek@saturn.yzu.edu.tw

Due to new regulations, the classic Sn-37Pb (wt.%) solder must be replaced by lead-free material. There are many alloys that could be used instead of this classic lead solder, including quaternary Ag-Cu-In-Sn alloy. The CALPHAD method was used for thermodynamic description of this quaternary system. Good agreement between calculation and available experimental information was found. Solidification of the promising lead-free solder Sn-1.5Ag-0.7Cu-9.5In (wt.%) was performed using the Scheil approach, and good agreement between this calculation and differential thermal analysis results was found. The obtained set of Gibbs energy functions can be used in the future for expanding the quaternary system to high-order ones.

Key words: Lead-free solder, CALPHAD approach, silver, copper, indium, tin

INTRODUCTION

Soldering technology is very important for the electronics industry. Recently, due to new regulations, the classic Sn-37Pb (wt.%) solder must be replaced by lead-free material. There are many candidates for use instead of this classic lead solder, including quaternary Ag-Cu-In-Sn alloy. This alloy was patented in Korea as a new type of solder with the following composition: "silver (Ag) of about 0.3 wt.% or more, and less than about 2.5 wt.%, copper (Cu) of about 0.2 wt.% or more, and less than about 2.0 wt.%, indium (In) of about 0.2 wt.% or more, and less than about 1.0 wt.% or less, and a balance of tin (Sn)."[1] There is the possibility of adding other components to the quaternary solder to obtain better properties, i.e., Ge or Al to improve antioxidation properties, or Bi or Zn to decrease the melting point of the solder. Taking into account all of these factors, it seems necessary to have a good thermodynamic description of the quaternary Ag-Cu-In-Sn system. The CALPHAD[2] method was used to carry out a thermodynamic assessment of this quaternary lead-free solder based on information available in the experimental literature.

(Received May 19, 2011; accepted August 30, 2011; published online October 1, 2011)

LITERATURE REVIEW

Thermodynamic properties and phase equilibrium data of the binary and ternary systems are available in the literature; however, there is a lack of information about the quaternary Ag-Cu-In-Sn system. The binary Ag-Cu system is a simple eutectic, and its description was taken from literature.[3] The Ag-In system includes, besides terminal phases, two solid solutions BCC_A2 and HCP_A3 and two intermetallic compounds Ag2Sn and AgIn2. The mixing enthalpy of the liquid phase was measured by Kleppa[4] at 723 K, by Castanet and Laffitte[5] at 745 K, by Nozaki[6] at 1100 K, by Beja[7] at 1028 K, and by Castanet at 1280 K. Activity of Ag in the liquid phase was measured by Alcock[8] at 1300 K. Alcock[8] also measured activity of In at the same temperature. Besides the work by Alcock,[8] the activity of In was measured by Qi[9] at 1300 K, by Jendrzejczyk et al.[10] at the temperature range between 948 K and 1328 K, and by Nozaki[11] at 1100 K. A thermodynamic investigation of the solid FCC_A1 phase was performed by Kleppa,[12] who measured the enthalpy of formation at 723 K, and by Masson,[13] who measured the chemical potential

of indium at 996 K. The liquidus/solidus and phase equilibria in solid state were determined by Moser et al.,[14] Weibke,[15] Campbell,[16] Hume-Rothery,[17] Owen,[18] and Staumanis.[19] The Ag-Sn system is similar to Ag-In and includes terminal FCC_A1(Ag) and BCT_A5(Sn), HCP_A3, and Ag3Sn phases. The enthalpies of mixing in the liquid phase were determined through calorimetric measurement by Kleppa[4] at 723 K, by Witting and Gehring[20] at 1248 K, by Laurie et al.[21] at 827 K, by Itagaki and Yazawa[22] at 1243 K, by Castanet et al.[23] at 1280 K, and by Rakotomavo et al.[24] at 1373 K. The chemical potentials of Ag in the liquid phase were examined using an electromotive force (EMF) measurement by Nozaki et al.[25] at 1100 K, by Okajima and Sako[26] in the temperature range 773 K to 893 K, by Laurie et al.[21] at 900 K, by Frantik and McDonald[27] at 900 K, by Yanko et al.[28] at 606 K and 685 K, by Elliot and Lemons[29] at 531 K to 525 K, by Chowdhury and Gosh[30] in the temperature range from 900 K to 1100 K, by Kubaschewski and Alcock[31] at 1180 K, by Fahri et al.[32] at 823 K, by Seetharaman and Staffanson[33] at 1073 K and 1373 K, by Iwase et al.[34] at 973 K, and by Kameda et al.[35] at 1173 K. Yamaji and Kato[36] at 1423 used the Knudsen cell technique combined with mass spectrometry analysis for determination of Ag activities in the liquid phase. The heat of formation of the FCC_A1(Ag), HCP_A3, and Ag3Sn phases were determined by the calorimetric method by Kleppa,[4] Witting and Gehring,[20] and by Laurie et al.[21] The heat capacities of the Ag3Sn phase were determined by Wallbrecht et al.[37] The liquidus/solidus and phase equilibria in the binary Ag-Sn system were determined by Heycock and Neville,[38] Murphy,[39] Petrenko,[40] Hume-Rothery and Reynolds,[41] and Umansky.[42] The binary Cu-In system is more complicated than previously described binaries. Besides terminal FCC_A1(Cu) and Tetragonal_A6(In), the system includes BCC_A2, CUIN_DELTA, CUIN_GAMMA, CUIN_ETA, and CUIN_THETA. The thermodynamic properties of the liquid were described by many researchers. The mixing enthalpy of the liquid phase was measured by Kleppa[43] at 723 K, by Beja[44] at 999 K, by Azakami and Yazawa[45] at 1273, by Itagaki and Yazawa[46] at 1373 K, by Kang et al.[47] at the temperature range from 903 K to 1348 K, and by Kang et al.[48] at 1373. The activities of components were determined by Azakami and Yazawa[45] at 1273 K, by Jagannathan and Gosh[49] at 1073 K, by Kang et al.[48] at 1373, and by Jacob and Alcock[50] at 900 K. The phase equilibria in the binary Cu-In system were investigated by Weibke and Eggers,[51] Hume-Rothery et al.,[52] Reynolds et al.,[53] Jain et al.,[54] Owen and Morris,[55] Jones and Owen,[56] Straumanis and Yu,[57] Walbrecht et al.,[58] Koster et al.,[59] and Vrojlik and Wolf.[60]

The enthalpies of mixing in the liquid Cu-Sn alloys were obtained using calorimetry by Kleppa[61] at 723 K, by Hultgren et al.[62] at 1400 K, by Takeuchi et al.[63] at 1363 K, by Yazawa and Itagaki[64] at 1373 K, by Iguchi et al.[65] at 1393 K, and by Pool et al.[66] and Lee et al.[67] at 997 K. The activities of Cu and Sn were measured by Alcock et al.,[68] Hager et al.,[69] and Ono et al.[70] using a Knudsen cell technique at 1300 K, 1593 K, and 1573 K, respectively. EMF measurements with the electrochemical cell technique were used by Oshi et al.[71] between 1173 and 1373 K and by Sengupta et al.[72] at 1073 K. All authors obtained activities of Cu and Sn with negative deviation from Raoult's law. Alcock and Jacob[73] used a gas–solid equilibration technique to measure the chemical potential of Sn in the terminal solid solution of Cu-side at 1000 K. Sommer et al.[74] and Predel and Schallner[75] used an EMF technique to measure the same variable at 1000 K. The phase diagram was investigated by Mamasumi and Takamoto,[76] Mamasumi,[77] Heycock and Neville,[78] Bauer and Vollenbruck,[79] Stockdale,[80] Raper,[81] Vero,[82] Haase and Pawlek,[83] and Bastow and Kirwood.[84]

The binary In-Sn system includes five phases: terminal BCT_A5(Sn) and Tetragonal_A6(In), two intermediate phases, and liquid. The description of this system was taken from literature.[85,86]

The quaternary Ag-Cu-In-Sn system includes four ternary systems: Ag-In-Sn, Ag-Cu-In, Ag-In-Sn, and Cu-In-Sn. These ternary systems have been investigated as well as binaries, and experimental information has been published. The thermodynamic properties of the liquid phase of the ternary Ag-In-Sn were investigated using calorimetric method by Gather et al.,[87] Alaoui-Elbelghiti,[88] and Luef et al.[89] The activities of the elements in liquid Ag-In-Sn alloys were determined by Miki et al.,[90] Popovic and Bencze,[91] and Jendrzejczyk et al.[92] The phase equilibria data were obtained by Liu et al.[93] Thermodynamic properties of the liquid Ag-Cu-Sn

Table I. Crystal structures of the phases in the quaternary Ag-Cu-In-Sn system

Phase	*Strukturbericht* Designation	Pearson Symbol	Space Group
FCC	A1	*cF*4	$Fm\bar{3}m$
BCC	A2	*cI*2	$Im\bar{3}m$
HCP	A3	*hP*2	$P6_3/mmc$
Ag2In		*cP*52	$P\bar{4}3m$
AgIn2		*tI*12	$I4/mcm$
Tetragonal	A6	*tI*2	$I4/mmm$
Ag3Sn		*oP*8	$Pmmm$
BCT	A5	*tI*4	$I4_1/amd$
CUIN_GAMMA		*cP*52	$P\bar{4}3m$
CUIN_DELTA		*aP*40	$P\bar{1}$
CUIN_ETA		*hP*4	$P6_3/mmc$
CUIN_THETA		*mC*20	$C2/m$
CUSN_EPSILON		*oC*80	$Cmcm$
CUSN_DELTA		*cF*416	$F\bar{4}3m$
CUSN_ZHETA		*hP*26	$P6_3$
INSN4		*tI*2	$I4/mmm$
IN3SN		*hP*5	$P6_3/mmm$

Table II. Calculated interaction parameters of the phases in the quaternary Ag-Cu-In-Sn system

Phase	Interaction Parameters	Comment
AgIn2	${}^{0}G^{\mathrm{AgIn2}}_{\mathrm{Ag:In}} = -8019.175 + 8.1980 * T + 0.33 * \mathrm{GHSERAG} + 0.67 * \mathrm{GHSERIN}$	This work
Ag3Sn	${}^{0}G^{\mathrm{Ag3Sn}}_{\mathrm{Ag:Ag}} = 4825.300 + 25.2970 * T + \mathrm{GHSERAG}$	This work
	${}^{0}G^{\mathrm{Ag3Sn}}_{\mathrm{Ag:Sn}} = -3976.0228 - 2.3632 * T + .75 * \mathrm{GHSERAG} + .25 * \mathrm{GHSERSN}$	This work
	${}^{0}G^{\mathrm{Ag3Sn}}_{\mathrm{Sn:Sn}} = 4.9583.968 + 0.07999 * T + \mathrm{GHSERSN}$	This work
	${}^{0}G^{\mathrm{Ag3Sn}}_{\mathrm{Cu:Sn}} = 500 + .75 * \mathrm{GHSERCU} + .25 * \mathrm{GHSERSN}$	This work
	${}^{0}L^{\mathrm{Ag3Sn}}_{*:\mathrm{Ag,Sn}} = -7652.6580 - 19.91374$	This work
	${}^{0}L^{\mathrm{Ag3Sn}}_{\mathrm{Ag,Cu:Sn}} = 3 * T$	This work
BCC_A2	${}^{0}L^{\mathrm{BCC\_A2}}_{\mathrm{Ag,Sn:Va}} = 7000$	This work
	${}^{0}L^{\mathrm{BCC\_A2}}_{\mathrm{Ag,Cu:Va}} = 36772.58 - 11.028 * T$	3
	${}^{1}L^{\mathrm{BCC\_A2}}_{\mathrm{Ag,Cu:Va}} = -4612.43 + .2887 * T$	3
	${}^{0}L^{\mathrm{BCC\_A2}}_{\mathrm{Ag,In:Va}} = 2858.3219 - 14.058972 * T$	This work
	${}^{1}L^{\mathrm{BCC\_A2}}_{\mathrm{Ag,In:Va}} = -76076.662 + 12.307714 * T$	This work
	${}^{2}L^{\mathrm{BCC\_A2}}_{\mathrm{Ag,In:Va}} = 31125.082$	This work
	${}^{0}L^{\mathrm{BCC\_A2}}_{\mathrm{Cu,Sn:V}} = 5497.236 - 22.307629 * T$	This work
	${}^{1}L^{\mathrm{BCC\_A2}}_{\mathrm{Cu,Sn:Va}} = -77713.554 + 60.253852 * T$	This work
	${}^{2}L^{\mathrm{BCC\_A2}}_{\mathrm{Cu,Sn:Va}} = -1.7331946 - 19.200183 * T$	This work
	${}^{0}L^{\mathrm{BCC\_A2}}_{\mathrm{Cu,In:Va}} = -20532.763 + 12.724 * T$	115
	${}^{1}L^{\mathrm{BCC\_A2}}_{\mathrm{Cu,In:Va}} = -13379.27 - 12.358 * T$	115
	${}^{0}L^{\mathrm{BCC\_A2}}_{\mathrm{Ag,Cu,Sn:Va}} = -9500$	This work
	${}^{1}L^{\mathrm{BCC\_A2}}_{\mathrm{Ag,Cu,Sn:Va}} = -242000 - 8 * T$	This work
	${}^{2}L^{\mathrm{BCC\_A2}}_{\mathrm{Ag,Cu,Sn:Va}} = 9500$	This work
	${}^{0}L^{\mathrm{BCC\_A2}}_{\mathrm{Ag,Cu,In:Va}} = 125000 + 45 * T$	This work
	${}^{1}L^{\mathrm{BCC\_A2}}_{\mathrm{Ag,Cu,In:Va}} = -696626 + 502.04 * T$	This work
	${}^{2}L^{\mathrm{BCC\_A2}}_{\mathrm{Ag,Cu,In:Va}} = -109889$	This work
	${}^{012}L^{\mathrm{BCC\_A2}}_{\mathrm{Cu,In,Sn:Va}} = 20000 + 5 * T$	This work
BCT_A5	${}^{0}L^{\mathrm{BCT\_A5}}_{\mathrm{Ag,Sn}} = 18358.8$	115
	${}^{0}L^{\mathrm{BCT\_A5}}_{\mathrm{Ag,In}} = -5000$	115
	${}^{0}L^{\mathrm{BCT\_A5}}_{\mathrm{In,Sn}} = -239 + 2.85 * T$	85,86
CUSN_ZHETA	${}^{0}G^{\mathrm{CUSN\_ZHETA}}_{\mathrm{Cu:Sn}} = -7080.1944 - 0.95536 * T + 0.769 * \mathrm{GHSERCU} + 0.231 * \mathrm{GHSERSN}$	This work
CUSN_EPSILON	${}^{0}G^{\mathrm{CUSN\_EPSILON}}_{\mathrm{Cu:Sn}} = -8453.7781 + .093538342 * T + .75 * \mathrm{GHSERCU} + .25 * \mathrm{GHSERSN}$	This work
	${}^{0}G^{\mathrm{CUSN\_EPSILON}}_{\mathrm{Cu:In}} = -6900 + 4 * T + .75 * \mathrm{GHSERCU} + .25 * \mathrm{GHSERIN}$	This work
	${}^{0}G^{\mathrm{CUSN\_EPSILON}}_{\mathrm{Ag:Sn}} = 5000 + .75 * \mathrm{GHSERAG} + .25 * \mathrm{GHSERIN}$	This work
	${}^{0}L^{\mathrm{CUSN\_EPSILON}}_{\mathrm{Cu:In,Sn}} = -10732.0016 + 12.2285706 * T$	This work
	${}^{0}L^{\mathrm{CUSN\_EPSILON}}_{\mathrm{Cu,Ag:Sn}} = 500$	This work
CUSN_DELTA	${}^{0}G^{\mathrm{CUSN\_DELTA}}_{\mathrm{Cu:Sn}} = -6498.0861 - 1.0645957 * T + .788 * \mathrm{GHSERCU} + .212 * \mathrm{GHSERSN}$	This work
	${}^{0}G^{\mathrm{CUSN\_DELTA}}_{\mathrm{Cu:In}} = -5350 + 1.5 * T + .788 * \mathrm{GHSERCU} + .212 * \mathrm{GHSERIN}$	This work

Table II. Continued

Phase	Interaction Parameters	Comment
	${}^{0}G^{\text{CUSN\_DELTA}}_{\text{Ag:Sn}} = 6000 + .788 * \text{GHSERAG} + .212 * \text{GHSERSN}$	This work
	${}^{0}L^{\text{CUSN\_EPSILON}}_{\text{Cu:In,Sn}} = -10732.0016 + 12.2285706 * T$	This work
	${}^{0}L^{\text{CUSN\_EPSILON}}_{\text{Cu,Ag:Sn}} = -50 + 8 * T$	This work
	${}^{0}L^{\text{CUSN\_EPSILON}}_{\text{Cu:In,Sn}} = -13000 + 14.77 * T$	This work
CUIN_DELTA	${}^{0}G^{\text{CUIN\_DELTA}}_{\text{Cu:Ag}} = +20000 + 5\text{*T} + .7 * \text{GHSERIN} + .3 * \text{GHSERAG}$	This work
	${}^{0}G^{\text{CUIN\_DELTA}}_{\text{Cu:In}} = -7991.308 + 1.1703 * \text{T} + .7 * \text{GHSERCU} + .3 * \text{GHSERIN}$	115
	${}^{0}G^{\text{CUIN\_DELTA}}_{\text{Cu:Sn}} = -5200 + .5 * T + .7 * \text{GHSERCU\#} + .3 * \text{GHSERSN}$	This work
	${}^{0}L^{\text{CUIN\_DELTA}}_{\text{Cu:Ag,In}} = -10000 + 10 * T$	This work
	${}^{0}L^{\text{CUIN\_DELTA}}_{\text{Cu:Sn,In}} = -13800 + 10.5 * T$	This work
CUIN_ETA	${}^{0}G^{\text{CUIN\_ETA}}_{\text{Cu:In}} = -8173.8 + 1.38 * T + .64 * \text{GHSERCU} + .36 * \text{GHSERIN}$	115
CUIN_GAMMA	${}^{0}G^{\text{CUIN\_GAMMA}}_{\text{Ag:In:Cu}} = +200 + .654 * \text{GHSERAG} + .231 * \text{GHSERIN} + .115 * \text{GHSERCU}$	115
	${}^{0}G^{\text{CUIN\_GAMMA}}_{\text{Ag:Ag:In}} = -1620.0692 - 6.5712402 * T + .769 * \text{GHSERAG} + .231 * \text{GHSERIN}$	115
	${}^{0}G^{\text{CUIN\_GAMMA}}_{\text{Cu:Cu:In}} = -2204.82 - 3.446 * T + .769 * \text{GHSERCU} + .231 * \text{GHSERIN}$	115
	${}^{0}G^{\text{CUIN\_GAMMA}}_{\text{Ag:In:In}} = +200 + .654 * \text{GHSERAG} + .346 * \text{GHSERIN}$	115
	${}^{0}G^{\text{CUIN\_GAMMA}}_{\text{Cu:In:In}} = -7131.647 + .11183 * T + .654 * \text{GHSERCU} + .346 * \text{GHSERIN}$	115
	${}^{0}G^{\text{CUIN\_GAMMA}}_{\text{Cu:Cu:Sn}} = -7900 + 5.43113 * T + .769 * \text{GHSERCU} + .231 * \text{GHSERSN}$	115
	${}^{0}G^{\text{CUIN\_GAMMA}}_{\text{Cu:In:Sn}} = +3144.8 - 2.4 * T + .654 * \text{GHSERCU} + .115 * \text{GHSERIN} + .231 * \text{GHSERSN}$	115
	${}^{0}L^{\text{CUIN\_GAMMA}}_{\text{Ag:Ag,In:In}} = -8456.9907 + 9.1311971 * T$	115
	${}^{0}L^{\text{CUIN\_GAMMA}}_{\text{Ag,Cu:Cu:In}} = -46000 - 25 * \text{T}$	115
	${}^{0}L^{\text{CUIN\_GAMMA}}_{\text{Ag,Cu:In:In}} = -2000$	115
	${}^{0}L^{\text{CUIN\_GAMMA}}_{\text{Cu:Cu,In::Sn}} = -12000$	115
Ag2In	${}^{0}G^{\text{Ag2In}}_{\text{Ag:Ag:In}} = -1620.0692 - 6.5712402 * T + .769 * \text{GHSERAG} + .231 * \text{GHSERIN}$	This work
	${}^{0}G^{\text{Ag2In}}_{\text{Ag:In:In}} = 7294.3897 - 1.7583637 * T + .654 * \text{GHSERAG} + .346 * \text{GHSERIN}$	This work
	${}^{0}L^{\text{Ag2In}}_{\text{Ag:Ag,In::In}} = -8456.9907 + 9.1311971 * T$	This work
CUIN_THETA	${}^{0}G^{\text{CUIN\_THETA}}_{\text{Cu:In}} = -7525.6 + 1.703 * T + .55 * \text{GHSERCU} + .45 * \text{GHSERIN}$	115
ETA	${}^{0}G^{\text{ETA}}_{\text{Ag:Cu:In}} = 200 + .545 * \text{GHSERAG} + .333 * \text{GHSERIN} + .122 * \text{GHSERCU}$	This work
	${}^{0}G^{\text{ETA}}_{\text{Cu:Cu:In}} = -6301.497 - .9396 * \text{T} + .667 * \text{GHSERCU} + .333 * \text{GHSERIN}$	115
	${}^{0}G^{\text{ETA}}_{\text{Ag:Ag:In}} = 200 + .545 * \text{GHSERAG\#} + .455 * \text{GHSERIN}$	This work
	${}^{0}G^{\text{ETA}}_{\text{Cu:In:In}} = -156.679 - 7.0297 * \text{T} + .545 * \text{GHSERCU} + .455 * \text{GHSERIN}$	115
	${}^{0}G^{\text{ETA}}_{\text{Cu:Sn:In}} = 16000 + .545 * \text{GHSERCU} + .122 * \text{GHSERSN}$	115
	${}^{0}G^{\text{ETA}}_{\text{Cu:Cu:Sn}} = 3200 + 2\text{*T} + .667 * \text{GHSERCU} + .333 * \text{GHSERSN}$	This work

Table II. Continued

Phase	Interaction Parameters	Comment
	${}^{0}G^{\mathrm{ETA}}_{\mathrm{Cu:In:Sn}} = -2492 + 4{*}\mathrm{T} + .545 * \mathrm{GHSERCU} + .122 * \mathrm{GHSERIN}$	115
	${}^{0}G^{\mathrm{ETA}}_{\mathrm{Cu:Sn:Sn}} = -8036.2536 + 1.470841 * T + .545 * \mathrm{GHSERCU\#} + .455 * \mathrm{GHSERSN}$	This work
	${}^{0}L^{\mathrm{ETA}}_{\mathrm{Cu:Ag,Cu:In}} = -1000$	This work
	${}^{0}L^{\mathrm{ETA}}_{\mathrm{Ag,Cu:Cu:In}} = -10000$	This work
	${}^{0}L^{\mathrm{ETA}}_{\mathrm{Ag,Cu:In:In}} = -5000$	This work
	${}^{0}L^{\mathrm{ETA}}_{\mathrm{Cu:Cu,In:In}} = -14526.546 + 18.02 * T$	115
	${}^{0}L^{\mathrm{ETA}}_{\mathrm{Cu:Cu,Sn:In}} = -14526.546 + 18.02 * T$	115
	${}^{0}L^{\mathrm{ETA}}_{\mathrm{Cu:Cu,In:Sn}} = -19650.8 - .4 * T$	115
	${}^{0}L^{\mathrm{ETA}}_{\mathrm{Ag,Cu:In:In}} = -10000 - 2 * \mathrm{T}$	This work
	${}^{0}L^{\mathrm{ETA}}_{\mathrm{Cu:In,Sn:In}} = -8300$	115
	${}^{0}L^{\mathrm{ETA}}_{\mathrm{Cu:In:In,Sn}} = -44570 + 39.6 * T$	115
	${}^{0}L^{\mathrm{ETA}}_{\mathrm{Cu:Sn:In,Sn}} = -30000 + T$	115
	${}^{0}L^{\mathrm{ETA}}_{\mathrm{Cu:Cu:In,Sn}} = -14526.546 + 18.02 * T$	115
	${}^{0}L^{\mathrm{ETA}}_{\mathrm{Cu:Cu,Sn:Sn}} = -8300$	115
	${}^{0}L^{\mathrm{ETA}}_{\mathrm{Cu:In,Sn:Sn}} = -8300$	115
FCC_A1	${}^{0}L^{\mathrm{FCC\_A1}}_{\mathrm{Ag,Sn:Va}} = 745.45 + 11.498027 * T$	93
	${}^{1}L^{\mathrm{FCC\_A1}}_{\mathrm{Ag,Sn:Va}} = -36541.5$	93
	${}^{0}L^{\mathrm{FCC\_A1}}_{\mathrm{Ag,Cu:Va}} = 36772.58 - 11.02847 * T$	3
	${}^{1}L^{\mathrm{FCC\_A1}}_{\mathrm{Ag,Cu:Va}} = -4612.43 + .28869 * T$	3
	${}^{0}L^{\mathrm{FCC\_A1}}_{\mathrm{Ag,In:Va}} = -17978.868 + 10.392923 * T$	This work
	${}^{1}L^{\mathrm{FCC\_A1}}_{\mathrm{Ag,In:Va}} = -32794.133$	This work
	${}^{0}L^{\mathrm{FCC\_A1}}_{\mathrm{Cu,Sn:Va}} = -9933.9036 + 4.4738745 * T$	This work
	${}^{1}L^{\mathrm{FCC\_A1}}_{\mathrm{Cu,Sn:Va}} = -13626.091 - 1.0835894 * T$	This work
	${}^{0}L^{\mathrm{FCC\_A1}}_{\mathrm{Cu,In:Va}} = -6475.911 + 21.83 * T$	116
	${}^{1}L^{\mathrm{FCC\_A1}}_{\mathrm{Cu,In:Va}} = -29935.183 - 5.672 * T$	116
	${}^{2}L^{\mathrm{FCC\_A1}}_{\mathrm{Cu,In:Va}} = 47350.167 - 40.21 * T$	116
	${}^{0}L^{\mathrm{FCC\_A1}}_{\mathrm{In,Sn:Va}} = 25000$	116
	${}^{0}L^{\mathrm{FCC\_A1}}_{\mathrm{Ag,In,Sn:Va}} = 105437 - 27.156 * T$	116
	${}^{1}L^{\mathrm{FCC\_A1}}_{\mathrm{Ag,In,Sn:Va}} = 173115$	116
	${}^{2}L^{\mathrm{FCC\_A1}}_{\mathrm{Ag,In,Sn:Va}} = 121030$	116
HCP_A3	${}^{0}L^{\mathrm{HCP\_A3}}_{\mathrm{Ag,Sn:Va}} = +1046.1 + 10.23693 * T$	94
	${}^{1}L^{\mathrm{HCP\_A3}}_{\mathrm{Ag,Sn:Va}} = -40505.5$	94
	${}^{0}L^{\mathrm{HCP\_A3}}_{\mathrm{Ag,Cu:Va}} = +36772.58 - 11.02847 * T$	3
	${}^{1}L^{\mathrm{HCP\_A3}}_{\mathrm{Ag,Cu:Va}} = -4612.43 + .28869 * T$	3
	${}^{0}L^{\mathrm{HCP\_A3}}_{\mathrm{Ag,In:Va}} = -15502.468 + 9.1292187 * T$	This work
	${}^{1}L^{\mathrm{HCP\_A3}}_{\mathrm{Ag,In:Va}} = -60975.391 + 4.7230074 * T$	This work
	${}^{2}L^{\mathrm{HCP\_A3}}_{\mathrm{Ag,In:Va}} = 31769.287$	This work
	${}^{0}L^{\mathrm{HCP\_A3}}_{\mathrm{Cu,Sn:Va}} = 6000$	This work
	${}^{0}L^{\mathrm{HCP\_A3}}_{\mathrm{Cu,In:Va}} = 6000$	This work
	${}^{0}L^{\mathrm{HCP\_A3}}_{\mathrm{In,Sn:Va}} = 6000$	This work
	${}^{0}L^{\mathrm{HCP\_A3}}_{\mathrm{Ag,Cu,Sn:Va}} = -5000 - 100 * T$	This work
	${}^{1}L^{\mathrm{HCP\_A3}}_{\mathrm{Ag,Cu,Sn:Va}} = -5000$	This work
	${}^{2}L^{\mathrm{HCP\_A3}}_{\mathrm{Ag,Cu,Sn:Va}} = -5000$	This work

Table II. Continued

Phase	Interaction Parameters	Comment
	${}^{0}L^{\text{HCP\_A3}}_{\text{Ag,Cu,In:Va}} = 115299.39 + 22.292826 * T$	This work
	${}^{1}L^{\text{HCP\_A3}}_{\text{Ag,Cu,In:Va}} = 1095674 - 30.520297 * T$	This work
	${}^{2}L^{\text{HCP\_A3}}_{\text{Ag,Cu,In:Va}} = -257262.3 - 667.14836 * T$	This work
	${}^{0}L^{\text{HCP\_A3}}_{\text{Ag,In,Sn:Va}} = -656.763393 + 43.0596186 * T$	This work
	${}^{1}L^{\text{HCP\_A3}}_{\text{Ag,In,Sn:Va}} = 140413.7 + 1.20624218 * T$	This work
	${}^{2}L^{\text{HCP\_A3}}_{\text{Ag,In,Sn:Va}} = 222065.019 + 5.05139267 * T$	This work
IN3SN	${}^{0}G^{\text{IN3SN}}_{\text{In}} = \text{GHSERIN}$	85,86
	${}^{0}G^{\text{IN3SN}}_{\text{Sn}} = 5015 - 7.5 * T + \text{GHSERSN}$	85,86
	${}^{0}L^{\text{IN3SN}}_{\text{In,Sn}} = -235 - 3.6954 * T$	85,86
INSN4	${}^{0}G^{\text{INSN4}}_{\text{In}} = 10292.5 - 7.64 * T + \text{GHSERIN}$	85,86
	${}^{0}G^{\text{INSN4}}_{\text{Sn}} = 925.3 - 1.7562 * T + \text{GHSERSN}$	85,86
	${}^{0}L^{\text{INSN4}}_{\text{In,Sn}} = -15715.5 + 19.3402 * T$	85,86
Liquid	${}^{0}L^{\text{Liquid}}_{\text{Ag,Sn}} = -399.49 - 31.42004 * T + 3.081837 * T * \text{LN}(T)$	This work
	${}^{1}L^{\text{Liquid}}_{\text{Ag,Sn}} = -18150.65 + 5.87501 * T$	This work
	${}^{2}L^{\text{Liquid}}_{\text{Ag,Sn}} = -12009.03 + 5.18355 * T$	This work
	${}^{0}L^{\text{Liquid}}_{\text{Ag,Cu}} = 17384.37 - 4.46438 * T$	3
	${}^{1}L^{\text{Liquid}}_{\text{Ag,Cu}} = 1660.74 - 2.31516 * T$	3
	${}^{0}L^{\text{Liquid}}_{\text{Ag,In}} = -26499.412 + 66.148718 * T - 8.6214682 * T * \text{LN}(T)$	This work
	${}^{1}L^{\text{Liquid}}_{\text{Ag,In}} = -38058.4 + 143.60133 * T - 17.657918 * T * \text{LN}(T)$	This work
	${}^{2}L^{\text{Liquid}}_{\text{Ag,In}} = -16572.628 + 121.0128 * T - 15.89588 * T * \text{LN}(T)$	This work
	${}^{3}L^{\text{Liquid}}_{\text{Ag,In}} = 5791.2978$	This work
	${}^{0}L^{\text{Liquid}}_{\text{Cu,Sn}} = -15583.768 + 40.623909 * T - 5.6172208 * T * \text{LN}(T)$	This work
	${}^{1}L^{\text{Liquid}}_{\text{Cu,Sn}} = -27739.285 + 41.927049 * T - 4.4641876 * T * \text{LN}(T)$	This work
	${}^{2}L^{\text{Liquid}}_{\text{Cu,Sn}} = -13228.943 + .90582783 * T$	This work
	${}^{0}L^{\text{Liquid}}_{\text{Cu,In}} = -41564.79 + 238.616 * T - 29.827 * T * \text{LN}(T)$	115
	${}^{1}L^{\text{Liquid}}_{\text{Cu,In}} = -76057.785 + 371.306 * T - 44.944 * T * \text{LN}(T)$	115
	${}^{2}L^{\text{Liquid}}_{\text{Cu,In}} = -42076.516 + 192.395 * T - 23.281 * T * \text{LN}(T)$	115
	${}^{0}L^{\text{Liquid}}_{\text{In,Sn}} = -711 - 1.6934 * T$	85,86
	${}^{1}L^{\text{Liquid}}_{\text{In,Sn}} = -64 - 1.3592 * T$	85,86
	${}^{0}L^{\text{Liquid}}_{\text{Ag,Cu,Sn}} = -116624.959 + 17.5155423 * T$	This work
	${}^{1}L^{\text{Liquid}}_{\text{Ag,Cu,Sn}} = -225103.627 + 119.668943 * T$	This work
	${}^{2}L^{\text{Liquid}}_{\text{Ag,Cu,Sn}} = -15633.0018 + 22.0596232 * T$	This work
	${}^{0}L^{\text{Liquid}}_{\text{Ag,Cu,In}} = -98722.781 + 75.612556 * T$	This work
	${}^{1}L^{\text{Liquid}}_{\text{Ag,Cu,In}} = -103273.75 + 30.571767 * T$	This work
	${}^{2}L^{\text{Liquid}}_{\text{Ag,Cu,In}} = -8975.9543 - 178.04098 * T$	This work
	${}^{0}L^{\text{Liquid}}_{\text{Ag,In,Sn}} = 7.36134942E + 04 - 1.55406011E + 01 * T$	This work
	${}^{2}L^{\text{Liquid}}_{\text{Ag,In,Sn}} = 3.06207639E + 04 - 2.11136487E + 01 * T$	This work
	${}^{3}L^{\text{Liquid}}_{\text{Ag,In,Sn}} = 5.57090815E + 03 - 4.55983225E + 00 * T$	This work
	${}^{0}L^{\text{Liquid}}_{\text{Cu,In,Sn}} = 106241.403 - 90.8977807 * T$	This work
	${}^{1}L^{\text{Liquid}}_{\text{Cu,In,Sn}} = -7127.12001 + 44.9051173 * T$	This work
	${}^{2}L^{\text{Liquid}}_{\text{Cu,In,Sn}} = -3414.76133 + 17.3825783 * T$	This work

system were investigated by Luef et al.,[94] who used a calorimetric method, and by Kopyto et al.,[95] who determined the chemical potential of Sn using the electromotive force measurement method. The equilibria between phases in this ternary system were investigated by Gebhardt and Petzow,[97] Shen,[97] Shen et al.,[98] Fodotov,[99,100] Miller,[101] Chada et al.,[102] Moon et al.,[103] Loomans and Fine,[104] and Yen and Chen.[105] The ternary system Ag-Cu-In has not been investigated as much as other ternaries described in this work. The thermodynamic properties of the liquid phase were measured by Wierzbicka-Miernik,[106] who used electromotive measurement as well as calorimetric measurement. The phase equilibria in this system were determined by Gebhard and Dreher,[107,108] Woychik and Massalski,[109] and Bahari et al.[110] The fourth ternary system is Cu-In-Sn. Thermodynamic properties of the liquid phase were determined by Fitzner,[111] Jendrzejczyk-Handzlik et al.,[112] Popovic and Bencze,[113] who determined the activity of elements in the liquid phase, and Li et al.,[114] who measured the mixing enthalpy of the liquid phase. The phase equilibria of the ternary Cu-In-Sn system ware determined by Liu et al.[115] and Lin et al.[116]

The quaternary system Ag-Cu-In-Sn was examined only in a tin-rich corner by Sopousek et al.[117] as a potential solder material.

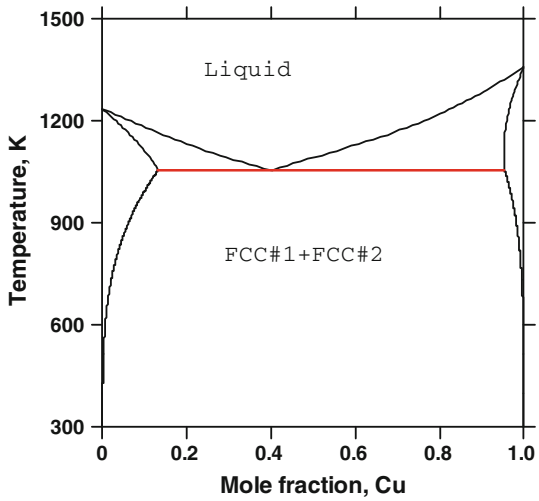

Fig. 1. Calculated system Ag-Cu.

THERMODYNAMIC MODELS

The following phases are considered in this work: FCC_A1, BCT_A5, BCC_A2, HCP_A3, Tetragonal_A6, IN3SN, INSN4 liquid, $Cu_{41}Sn_{11}$, $Cu_{10}Sn_3$, Cu_3Sn, Cu_6Sn_5, CUIN_DELTA, CUIN_ETA, CUIN_GAMMA, CUIN_THETA, AGIN2, AG2IN, and AGSB_ORTHO. Detailed information about these phases is given in Table I and below.

Substitutional Solution: FCC_A1, BCC_A2, BCT_A5, Liquid, Tetragonal_A6, INSN4, IN3SN

The Gibbs free energies of pure elements with respect to temperature ${}^0G_i(T) = G_i(T) - H_i^{SER}$ are represented by Eq. (1):

$$ {}^0G_i(T) = a + bT + cT\ln(T) + dT^2 + eT^{-1} + fT^3 + iT^4 + jT^7 + kT^{-x}. \quad (1) $$

The ${}^0G_i(T)$ data are referred to the constant enthalpy value of the standard element reference

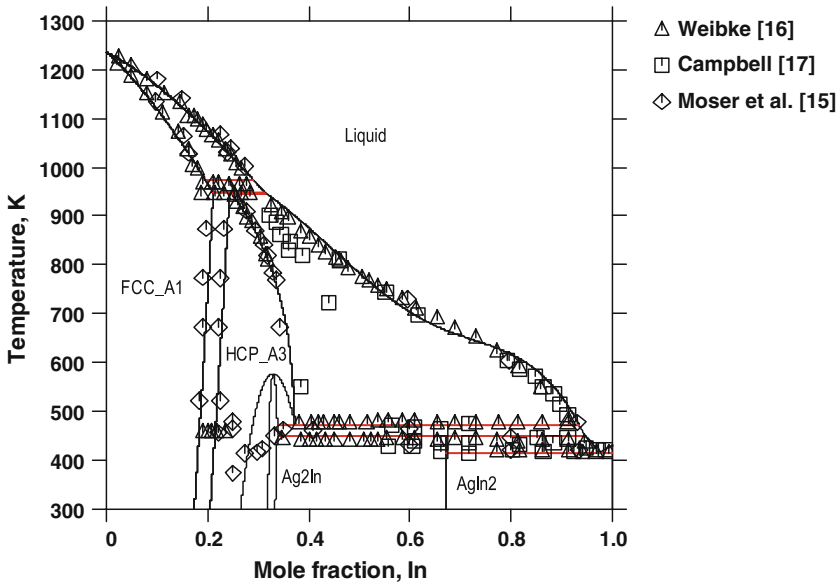

Fig. 2. Calculated binary Ag-In system.

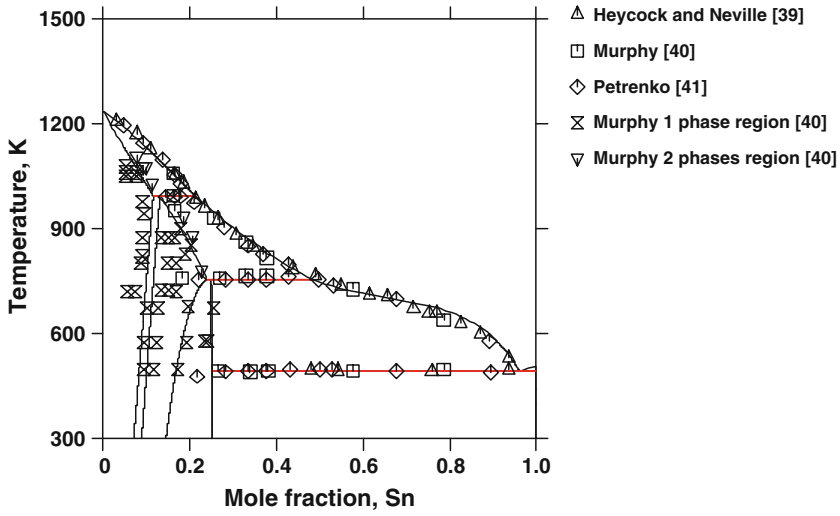

Fig. 3. Calculated binary Ag-Sn system.

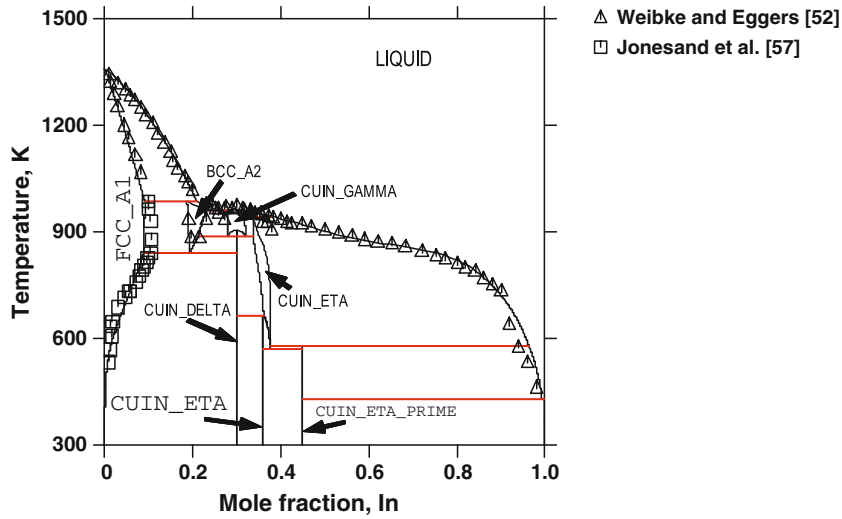

Fig. 4. Calculated binary Cu-In system.

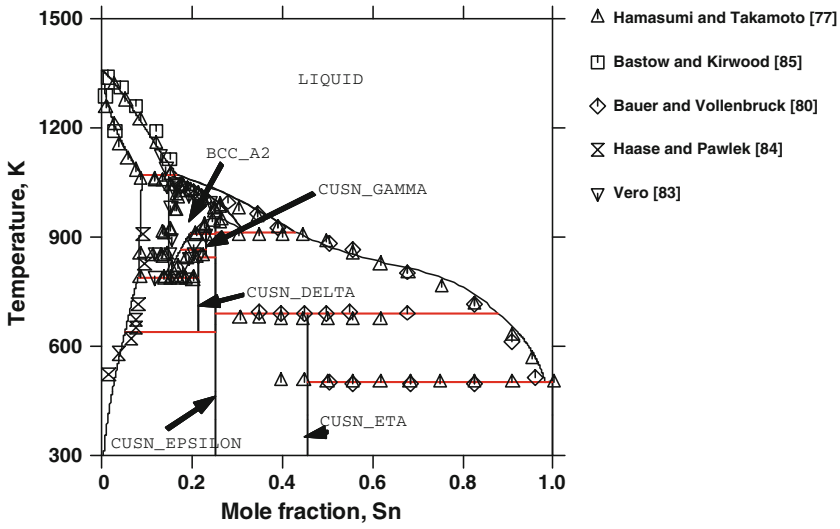

Fig. 5. Calculated binary Cu-Sn system.

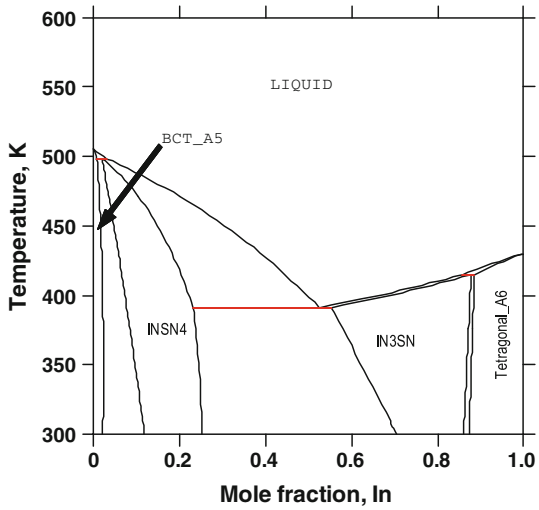

Fig. 6. Calculated binary In-Sn system.

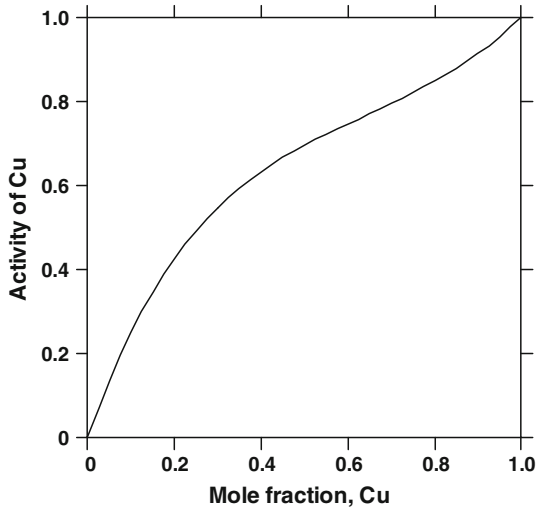

Fig. 7. Activity of Cu in liquid Ag-Cu at 1200 K.

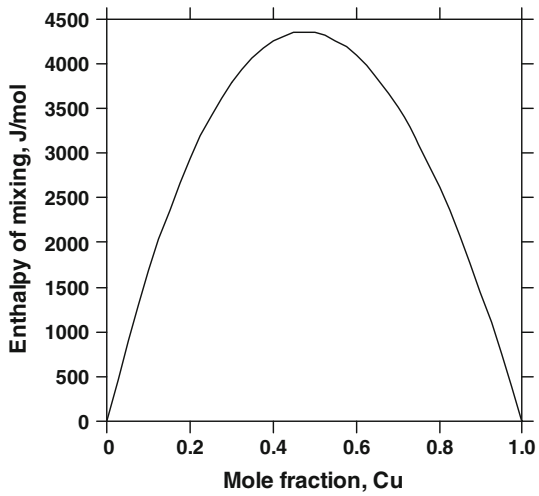

Fig. 8. Calculated enthalpy of mixing of liquid Ag-Cu at 1200 K.

H_i^{SER} at 298.15 K and 1 bar as recommended by Scientific Group Thermodata Europe (SGTE).[118] The reference states are: FCC_A1 (Cu nd Ag), BCT_A5 (Sn), and Tetragonal_A6(In). The ${}^0G_i(T)$ expression may be given for several temperature ranges, where the coefficients a, b, c, d, e, f, i, j, and k have different values. The ${}^0G_i(T)$ functions are taken from the SGTE unary (pure elements) thermodynamic database (TDB) v.4.[117] The thermodynamic functions of pure elements are listed in Table III. Solid and liquid solution phases (FCC_A1, BCC_A2, BCT_A5, HCP_A3, Tetragonal_A6, In3Sn, InSn4, and Liquid) are described by the regular solution model[119]:

$$G_m(T) = \sum_i x_i {}^0G_i(T) + RT\sum_i x_i \ln(x_i) + \sum_i \sum_{j>i} x_i x_j \left(\sum_v {}^vL_{ij}(x_i - x_j)^v \right), \quad (2)$$

where the $\sum_i \sum_{j>i} x_i x_j \left(\sum_v {}^vL_{ij}(x_i - x_j)^v \right)$ part is the Redlich–Kister polynomial for excess Gibbs free energy.

Stoichiometric Compounds

Binary stoichiometric compounds $Cu_{41}Sn_{11}$, $Cu_{10}Sn_3$, Cu_3Sn, Cu_6Sn_5, CUIN_DELTA, CUIN_THETA, $AgIn_2$, and AGSB_ORTHO are described as the line compound using the following:

$$G_m(T) = a + bT + \sum_i x_i GHSER_i. \quad (3)$$

CUIN_GAMMA

The phase CUIN_GAMMA is described by a compound energy model[121] using three sublattices: $(Cu)_{0.645}:(Cu,In)_{0.115}:(In)_{0.231}$

$$\begin{aligned} G_m^{CUIN\_GAMMA}(T) = {} & Y_{Cu}^{I} Y_{Cu}^{II} Y_{In}^{III} {}^0G_{Cu:Cu:In}^{CUIN\_GAMMA} \\ & + Y_{Cu}^{I} Y_{In}^{II} Y_{In}^{III} {}^0G_{Cu:In:In}^{CUIN\_GAMMA} \\ & + 0.115RT\left(Y_{Cu}^{II} \ln Y_{Cu}^{II} + Y_{In}^{II} \ln Y_{In}^{II}\right) \\ & + {}^{xs}G_m^{CUIN\_GAMMA}. \end{aligned} \quad (4)$$

CUIN_ETA

The phase CUIN_GAMMA is described by a compound energy model using three sublattices: $(Cu)_{0.545}:(Cu,In)_{0.122}:(In)_{0.333}$

$$\begin{aligned} G_m^{CUIN\_ETA}(T) = {} & Y_{Cu}^{I} Y_{Cu}^{II} Y_{In}^{III} {}^0G_{Cu:Cu:In}^{CUIN\_ETA} \\ & + Y_{Cu}^{I} Y_{In}^{II} Y_{In}^{III} {}^0G_{Cu:In:In}^{CUIN\_ETA} \\ & + 0.122RT\left(Y_{Cu}^{II} \ln Y_{Cu}^{II} + Y_{In}^{II} \ln Y_{In}^{II}\right) \\ & + {}^{xs}G_m^{CUIN\_ETA}. \end{aligned} \quad (5)$$

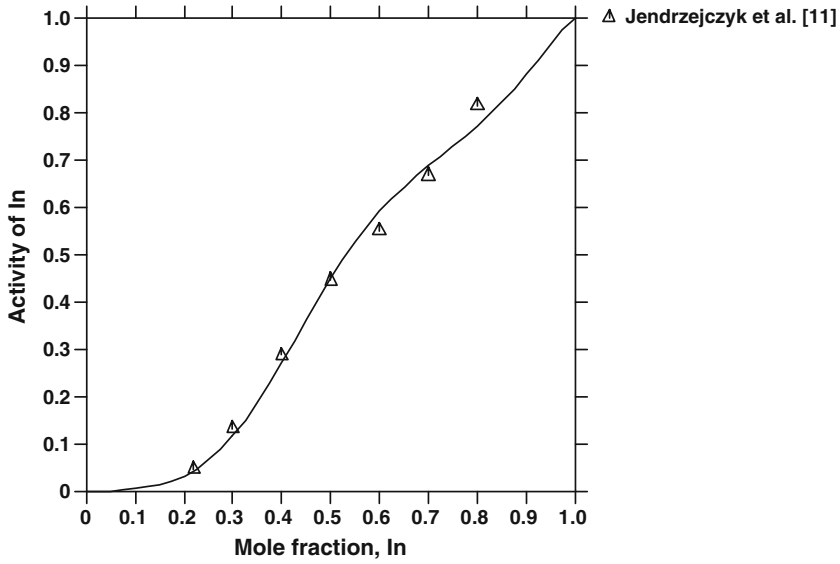

Fig. 9. Activity of In in liquid Ag-In at 1028 K.

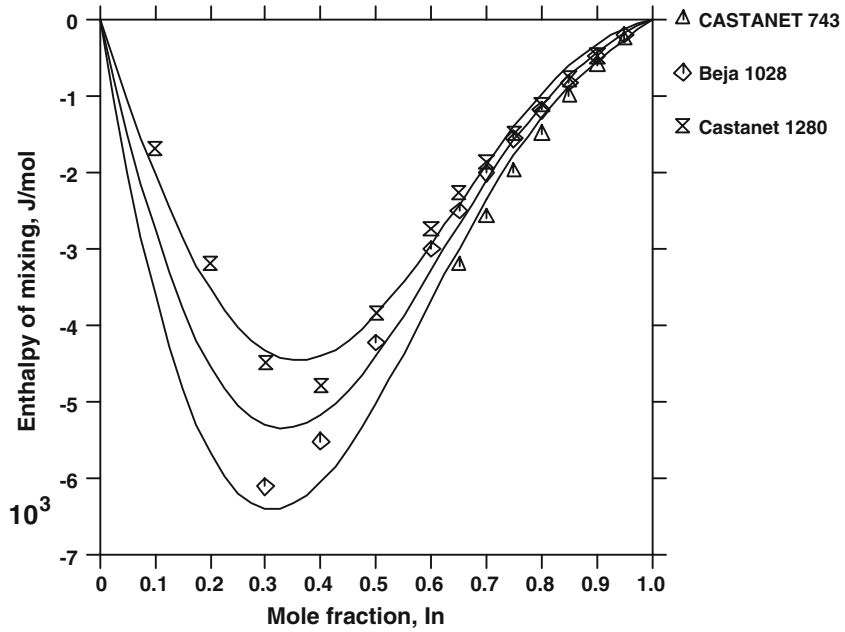

Fig. 10. Enthalpy of mixing of liquid Ag-In at different temperatures compared with experimental data.

AGIn2

The phase CUIN_GAMMA is described by a compound energy model using three sublattices: $(Ag)_{0.645}:(Ag,In)_{0.115}:(In)_{0.231}$

$$\begin{aligned} G_m^{AgIn2}(T) = {} & Y_{Ag}^{I} Y_{Ag}^{II} Y_{In}^{III0} G_{Ag:Ag:In}^{AgIn2} \\ & + Y_{Ag}^{I} Y_{In}^{II} Y_{In}^{III0} G_{Ag:In:In}^{AgIn2} \\ & + 0.115RT\left(Y_{Ag}^{II} \ln Y_{Ag}^{II} + Y_{In}^{II} \ln Y_{In}^{II}\right) \\ & + {}^{XS}G_m^{CUIN\_GAMMA}. \end{aligned} \quad (6)$$

MODELING PROCEDURE

The thermodynamic parameters for all phases in the system were optimized using ThermoCalc software.[121] For this optimization, thermodynamic data for the liquid phase, invariant reactions, liquidus/solidus, and solid-phase equilibria were used. Each piece of selected information was given a certain weight based on personal judgment. Optimization was carried out step by step in agreement with Schmid-Fetzer et al.'s[122] guideline. First, optimization of the liquid phase was performed, then the solid phases were assessed. All parameters were

finally evaluated together to provide the best description of the system. The calculated interaction parameters are shown in Table II. To check the results of optimization, the system was also calculated using Pandat software.[123]

RESULTS AND DISCUSSION

Calculated binary systems superimposed with experimental data are shown in Fig. 1a–f. Figure 1 exhibits calculated binary Ag-Cu system. The calculation was made based on Hayes et al.'s[3] proposition. Figure 2 shows calculated Ag-In binary system superimposed with experimental data obtained by Weibke,[15] Campbell,[16] and Moser et al.[14]

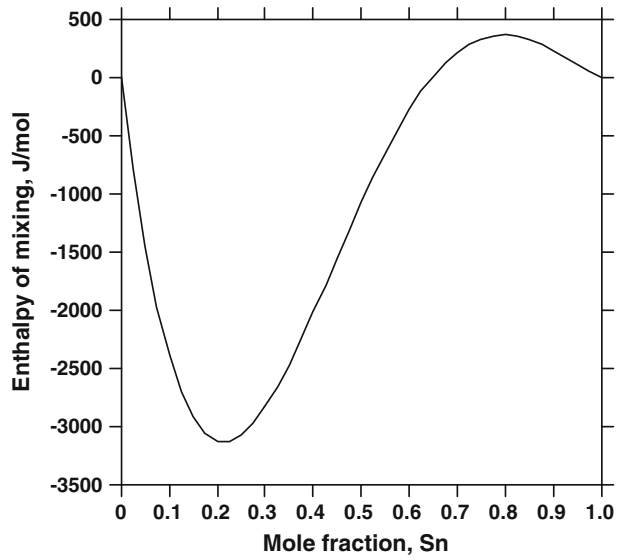

Fig. 11. Enthalpy of mixing of liquid Ag-Sn at 1173 K.

As can be seen from the figure, calculation reproduces experimental data well. Figure 3 displays binary Ag-Sn system together with experimental data obtained by Heycock and Neville,[38] Murphy,[39] and Petrenko.[40] The figure exhibits very good agreement between calculations and experiment. Figure 4 shows calculated phase diagram of the binary Cu-In system superimposed with data obtained by Weibke and Eggers[51] and Jones and Owen.[56] Very good agreement between calculation and experiment was obtained; however, for low concentration of indium, the calculated liquidus line lies slightly above the experimental data. The experimental information obtained by Weibke and Eggers[51] exhibits in this region less smooth characteristics than calculation. Figure 5 shows calculated binary Cu-Sn system with experimental data obtained by Hamasumi and Takamoto,[76] Bastow and Kirwood,[84] Bauer and Vollenbruck,[79] Haase and Pawlek,[83] and Vero.[82] The system Cu-Sn was simplified because of lack of information about the transformations GAMMA_DO3 → BCC_A2 and CUSN_ETA → CUSN_ETA_Prime in the ternary Cu-Sn-Me systems. In these cases, the region GAMMA_DO3 + BCC_A2 was modeled as BCC_A2, and the polymorphic transformation CUSN_ETA → CUSN_ETA_PRIME was neglected. From Fig. 5 one can see that the calculation agrees with experimental data well, even with this simplification. Figure 6 shows the calculated phase diagram of the binary In-Sn system based on the reports of Lee et al.[85] and Moelans.[86] Thermodynamic properties of the liquid phase of the binary systems are shown in Figs. 7–l8. Figures 7 and 8 show activity of Cu in liquid Ag-Cu at 1200 K and enthalpy of mixing of liquid Ag-Cu also at 1200 K. The activity of copper shows a positive deviation from Raoult's

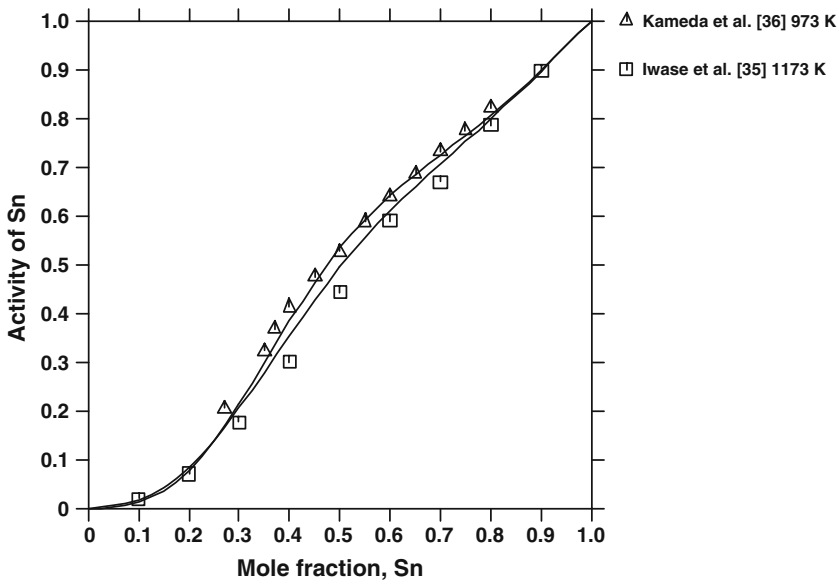

Fig. 12. Activity of Sn in liquid Ag-Sn at 973 K and 1173 K compared with experimental data.

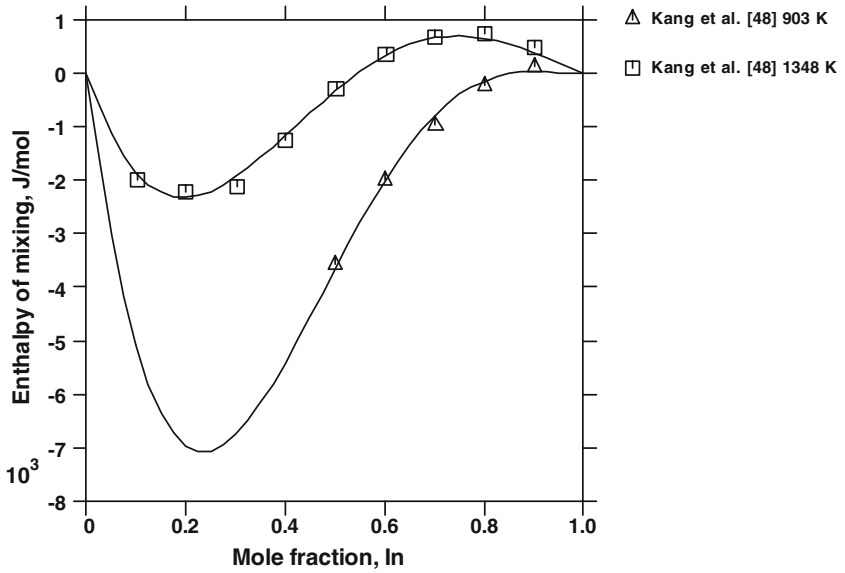

Fig. 13. Enthalpy of mixing of liquid Cu-In at 903 K and 1348 K superimposed with experimental data.

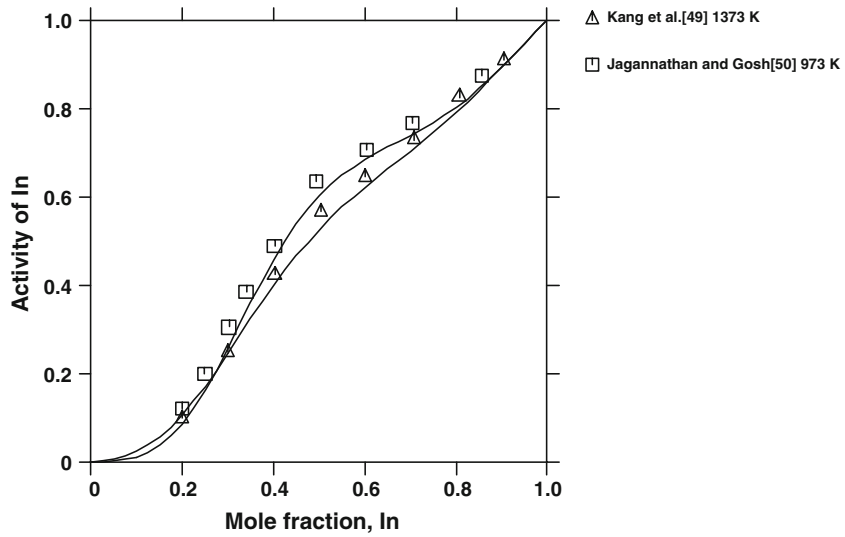

Fig. 14. Activity of In in liquid Cu-In at 1373 K and at 973 K together with experimental data.

law for the whole range of composition. This liquid phase exhibits positive heat effect without temperature dependency, which is shown in Fig. 8. Figure 9 displays activity of indium in liquid Ag-In alloy at 1028 K superimposed with experimental data obtained by Jendrzejczyk et al.[10] The activity shows a slightly negative deviation from Raoult's law. Next, Fig. 10 shows the calculated enthalpy of mixing of liquid Ag-In, which exhibits strong temperature dependency. Figure 11 displays the mixing enthalpy of liquid Ag-Sn at 1173 K. The enthalpy of mixing has negative values for low concentration of Sn and slightly positive ones for high concentration of tin. The activity of tin in liquid Ag-Sn at 973 K and 1173 K is shown in Fig. 12. From this figure it can be seen that experimental data obtained by Kameda et al.[35] and Iwase et al.[34] are reproduced well. Figure 13 shows the calculated enthalpy of mixing of liquid Cu-In together with experimental data obtained by Kang et al.[47] at 903 K and at 1348 K. It can be seen that the heat of mixing of liquid phase of the Cu-In system is strongly dependent on temperature. The activity of indium in the same system at temperatures of 973 K and 1373 K

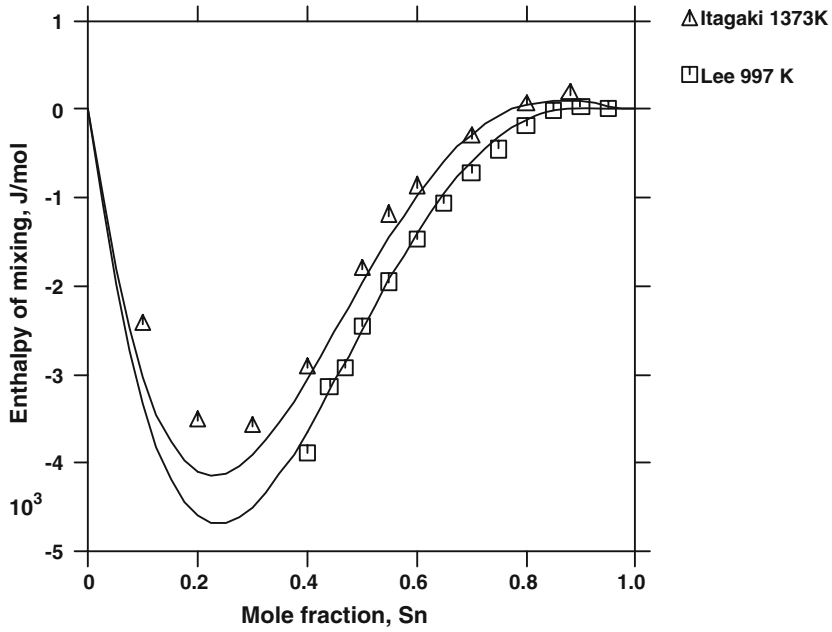

Fig. 15. Calculated enthalpy of mixing of liquid Cu-Sn compared with experimental data obtained by Itagaki[63] and Lee.[68]

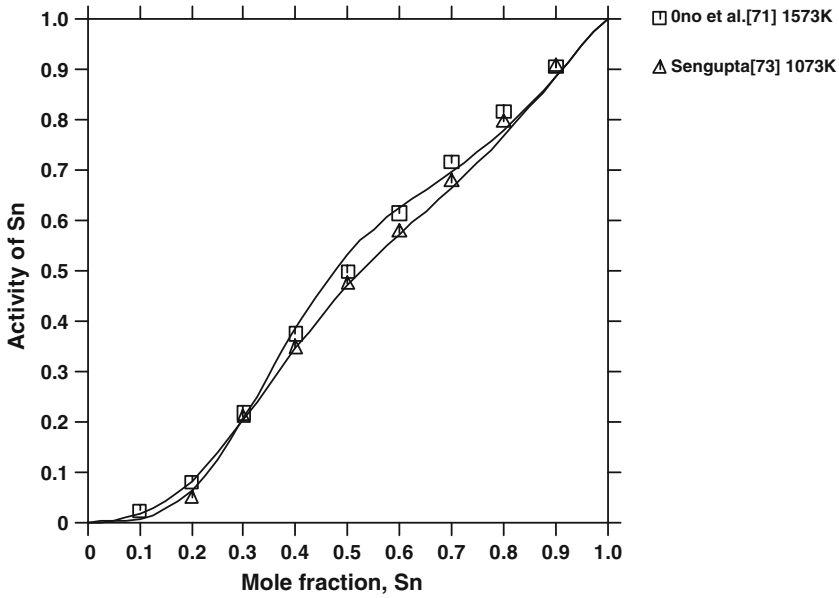

Fig. 16. Calculated activity of Sn in liquid Cu-Sn at 1073 and 1573 K together with experimental data.

together with experimental data obtained by Kang et al.[48] and Jagannathan and Gosh[49] is shown in Fig. 14. As can be seen from these figures, the thermodynamic properties of the liquid Cu-In are reproduced well by the description proposed in this work. Figure 15 displays the calculated enthalpy of mixing of the liquid Cu-Sn phase at 997 K and at 1373 K. The heat of mixing is slightly dependent on temperature, and the calculated functions agree well with experimental data proposed by Yazawa and Itagaki[64] and Lee.[67] Figure 16 shows the calculated activity of Sn in the liquid Cu-Sn system at 1073 K and at 1573 K together with experimental data measured by Ono et al.[70] and Sengupta et al.[72] The calculation agrees well with experimental data and shows only slight dependence on temperature.

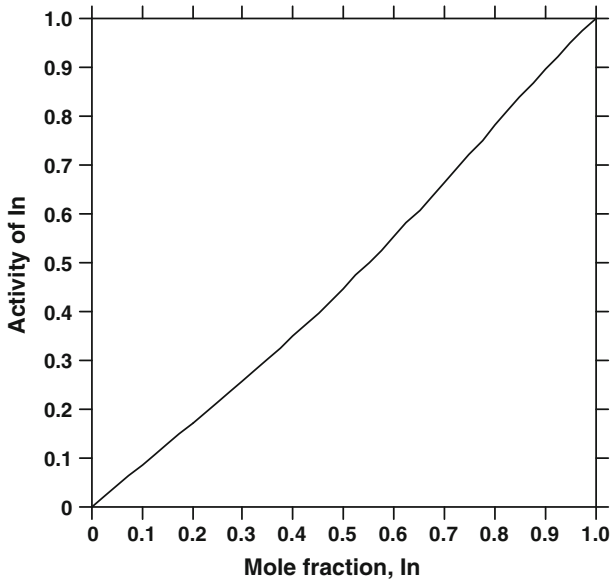

Fig. 17. Activity of In in liquid In-Sn at 1273 K.

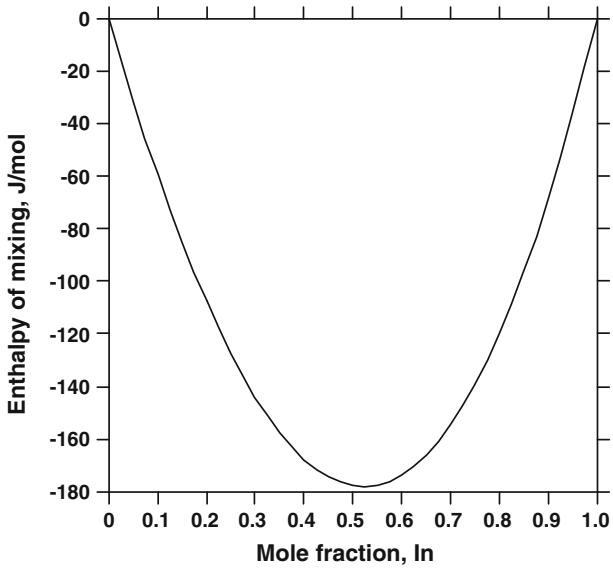

Fig. 18. Calculated enthalpy of mixing of liquid In-Sn at 1273 K.

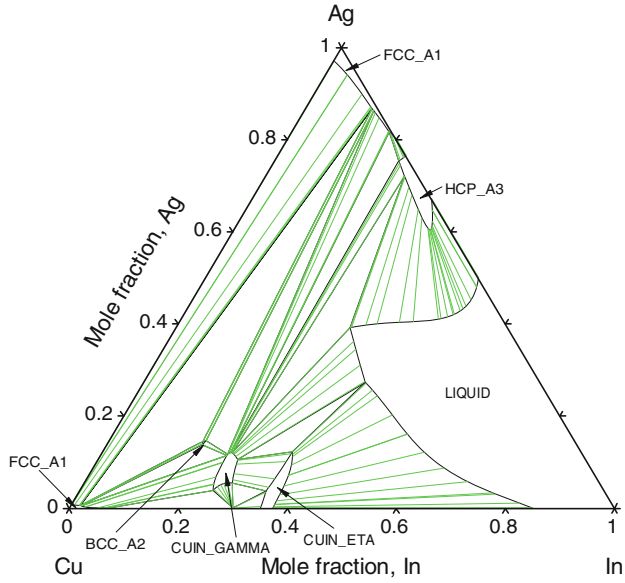

Fig. 19. Isothermal section of Ag-Cu-In system at 783 K.

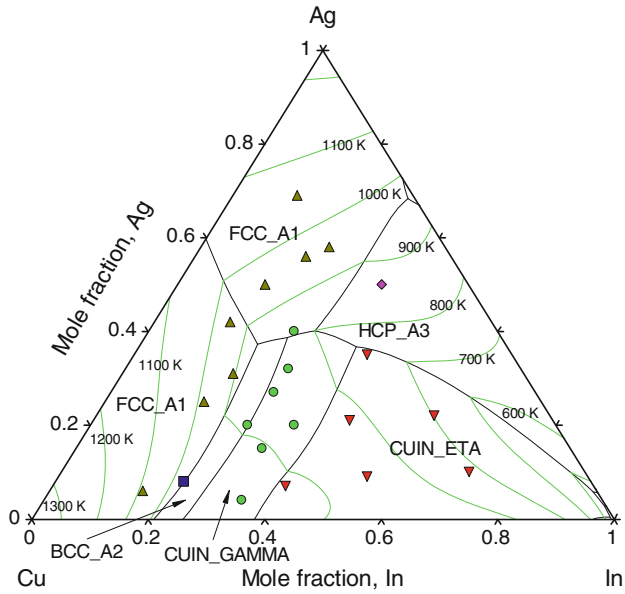

Fig. 20. Liquidus projection of the Ag-Cu-In system superimposed with experimental data obtained by Woychik and Massalski.[110]

Figures 17 and 18 show the calculated activity of In in liquid In-Sn at 1173 K and enthalpy of mixing of the liquid phase at the same temperature, respectively. The calculations were done using data obtained by Lee et al.[85] and Moelans et al.[86] Figure 19 shows the calculated isothermal section of the Ag-Cu-In system. The calculation agrees with Bahari et al.'s[109] work. There is a big difference between the phase equilibria presented in Bahari et al.[110] and those presented in Woychik and Massalski's[109] work. Woychik and Massalski showed that CUIN_GAMMA and Ag2In phases make a continuous solid solution through the whole system; however, Bahari et al.[110] presented that those phases are not even in equilibrium. Bahari et al.[110] proposed equilibrium between Ag2In, Cu11In9, and CUIN_ETA/ETA_prime and equilibrium between CUIN_GAMMA, HCP_A3, and FCC_A1(Cu). The different equilibrium between phases shown by these two works should motivate future work on the Ag-Cu-In ternary system. Figure 20 shows calculated liquidus projection of the ternary Ag-Cu-Sn system superimposed with data obtained by Woychik and Massalski[109] As can be seen from this figure, although

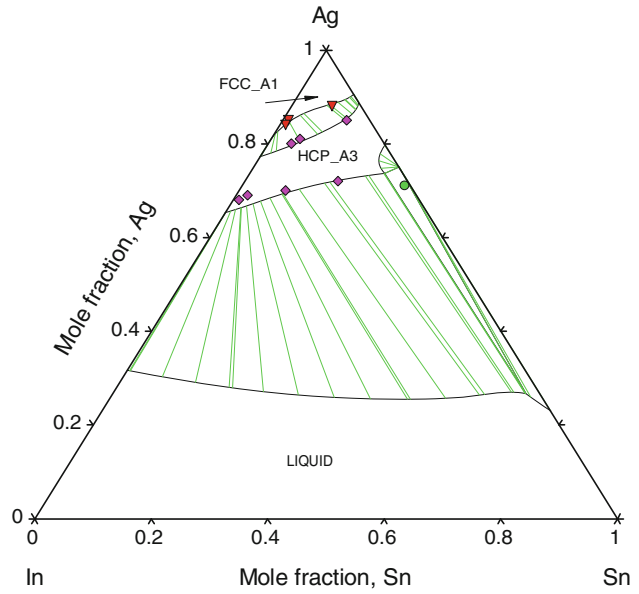

Fig. 21. Isothermal section of the Ag-In-Sn system at 673 K compared with experimental data obtained by Liu et al.[95]

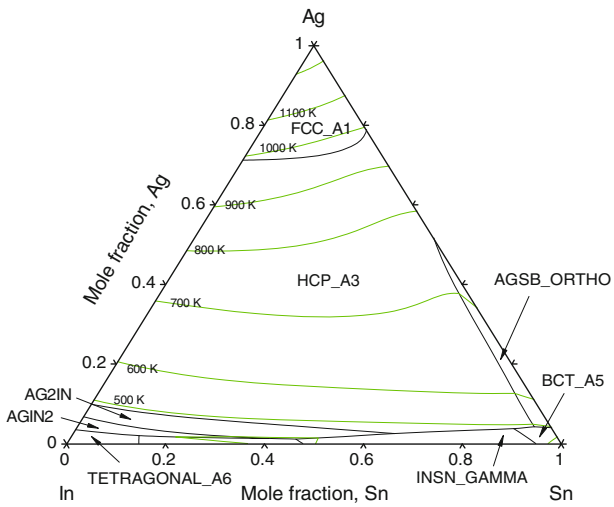

Fig. 22. Liquidus projection of the Ag-In-Sn system.

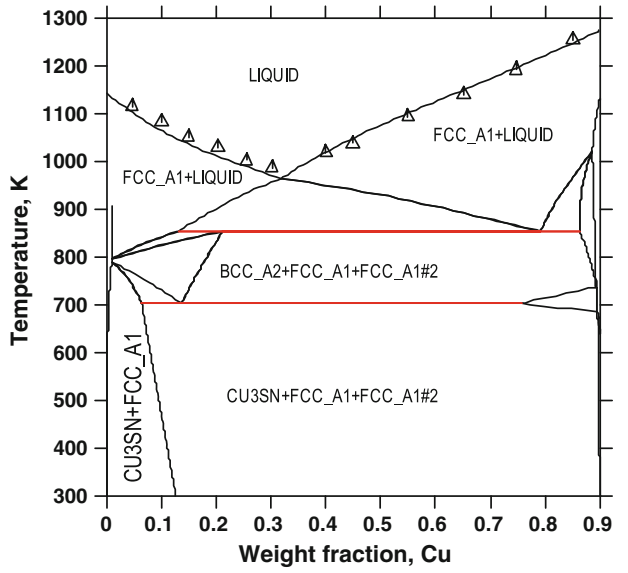

Fig. 23. Isoplethal section of the Ag-Cu-Sn system for constant concentration $w(Sn) = 0.1$ together with experimental data obtained by Gephard and Petzow.[96]

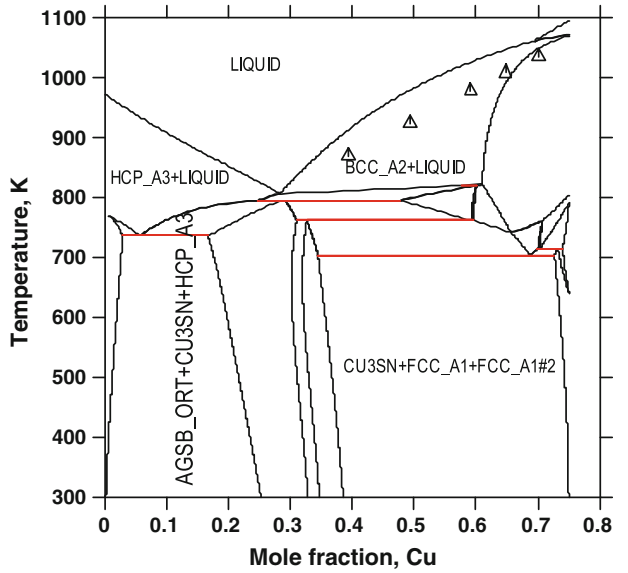

Fig. 24. Isoplethal section of the Ag-Cu-Sn system for constant concentration $w(Sn) = 0.25$ together with experimental data obtained by Gephard and Petzow.[96]

the phase equilibrium at 780 K agrees with Bahari et al.'s[110] work, the liquidus projection agrees with Woychik and Massalski's[109] data. Figures 21 and 22 show isothermal section at 673 K and liquidus projection of the ternary Ag-In-Sn system. The isothermal section is compared with data obtained by Liu et al.[115] From this figure, one can see that the calculation reproduced the experimental information well. Figure 22 shows the calculated liquidus projection of the ternary Ag-Cu-Sn system. Next, Figs. 23 and 24 display the calculated isopleth intersection for concentration of Sn equal to 0.1 and 0.25 weight fraction, respectively, together with information obtained by Gephard and Petzow.[96] The liquidus projection for the constant concentration of Sn of 0.1 weight fraction is reproduced very well. The calculated liquidus for concentration of Sn equal to 0.25 weight fraction lies slightly above experimental data; however, the description of the liquidus line in the binary Cu-Sn agrees with experimental data obtained for this binary system. Figure 25 exhibits isothermal section of this ternary

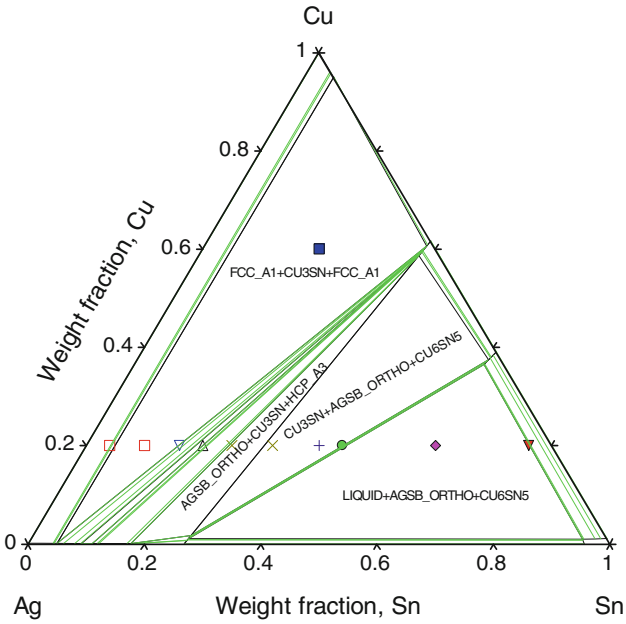

Fig. 25. Calculated isothermal section of the Ag-Cu-Sn system superimposed with experimental data obtained by Yen and Chen.[105]

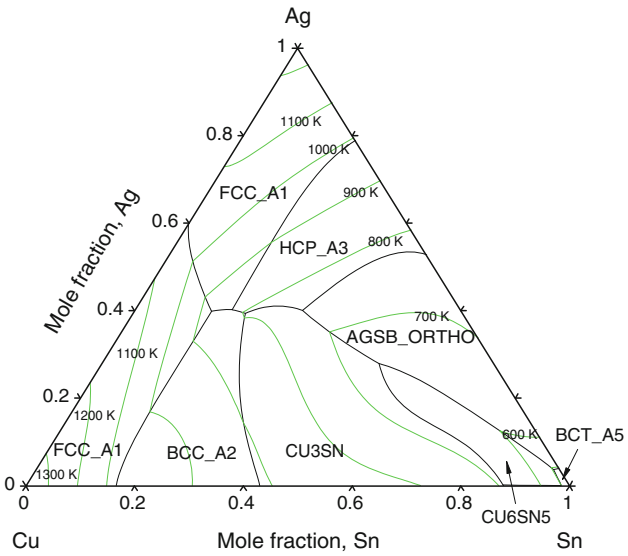

Fig. 26. Calculated liquidus projection of the Ag-Cu-Sn system.

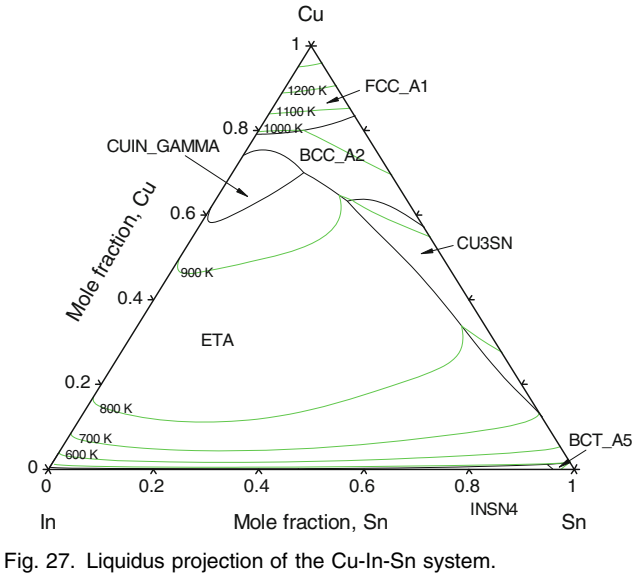

Fig. 27. Liquidus projection of the Cu-In-Sn system.

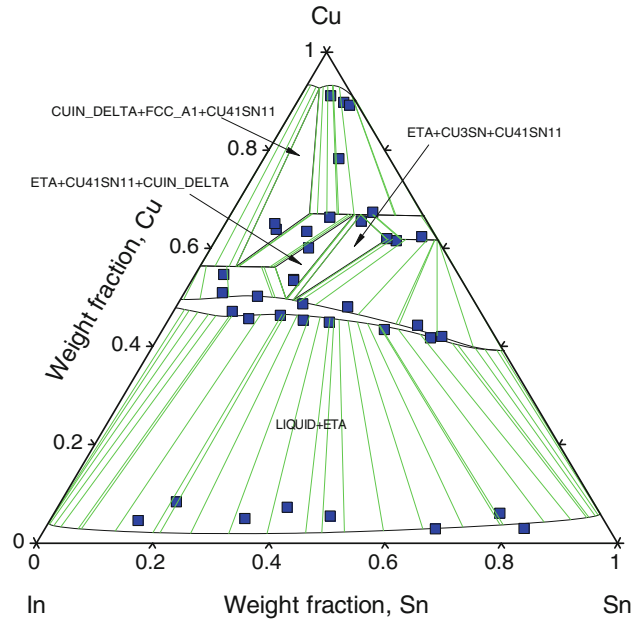

Fig. 28. Isothermal section of the Cu-In-Sn system at 673 K superimposed with data obtained by Liu et al.[115]

system together with data obtained by Yen and Chen[105] at 513 K. The calculated isothermal section shows good agreement with experimental data (Fig. 25). Generally speaking, the calculation of the isothermal section agrees with experimental data. The discrepancy can be found for the homogeneity range of FCC_A1 phase, which is larger in Yen and Chen's[105] work than it appears from calculations. Figure 26 shows calculated liquidus projection of the ternary Ag-Cu-Sn system. Figure 27 shows calculated liquidus projection of the ternary system Cu-In-Sn. Figure 28 presents calculated isothermal section of this ternary system together with experimental data obtained by Liu et al.[115] As can be seen from this figure, the isothermal section mostly agrees with the experimental information. However, with high concentration of copper, there is some discrepancy between the calculation and the experiment, which can be explained in two ways. The first reason for the discrepancy can be because a line compound model for intermetallic phases such as Cu3Sn is used. In this case, the homogeneity range of the compound is neglected and a line rep-

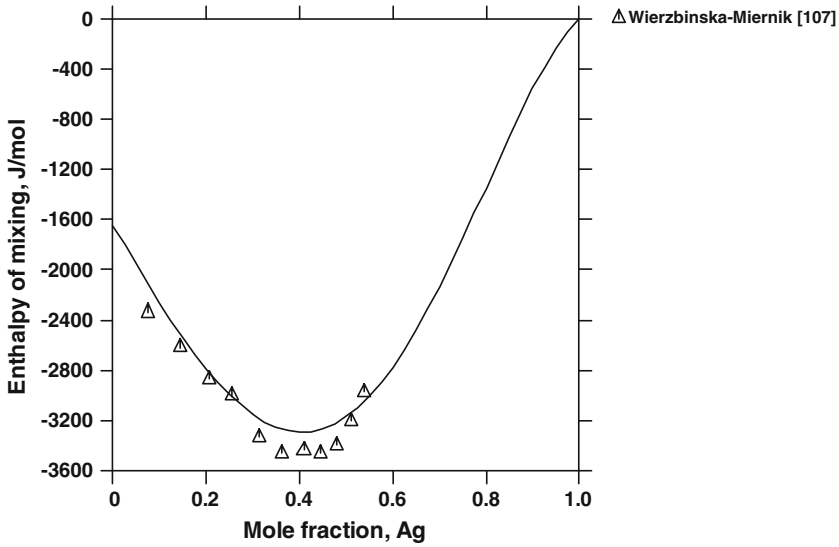

Fig. 29. Enthalpy of mixing of the liquid Ag-In-Sn at 1173 K for intersection $x(\mathrm{Cu}) = x(\mathrm{In})$ superimposed with experimental data obtained by Wierzbinska-Miernik.[106]

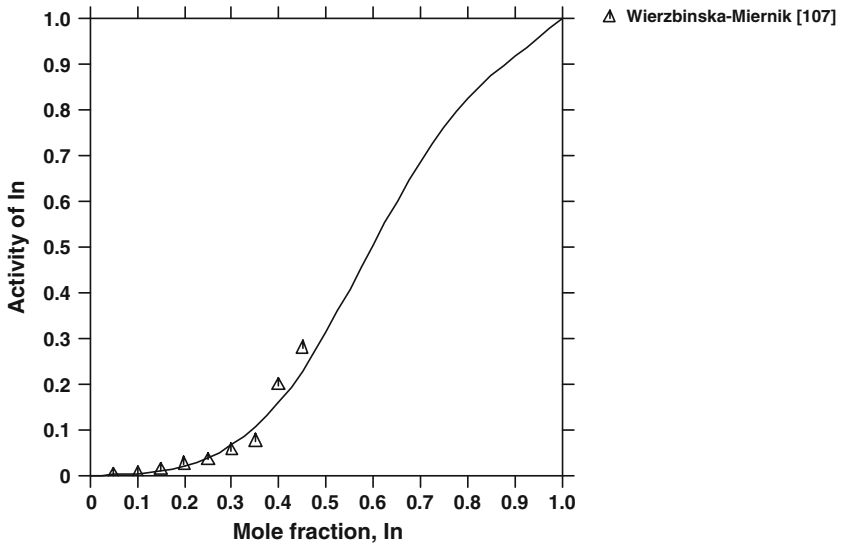

Fig. 30. Activity of In in liquid Ag-Cu-In at 1173 K for intersection $x(\mathrm{Ag}) - x(\mathrm{Cu}) = 0$ superimposed with experimental data obtained by Wierzbinska-Miernik.[106]

resents the intermetallic compound (IMC). The second reason can be due to the thermodynamic modeling of the phase Cu16In3Sn being omitted, which can be found at 673 K in Liu et al.'s[115] work. Unfortunately, there is no more information about this phase, and moreover, the phase does not appear at the isothermal sections determined for different temperatures. Taking into account the lack of information about the Cu16In3Sn intermetallic compound, this IMC was not included in the optimization procedure. Thermodynamic properties of the liquid phase of the ternary Ag-Cu-In system are shown in Figs. 29 and 30. Figure 29 displays the calculated mixing enthalpy of the liquid Ag-Cu-In alloy at 1173 K for an intersection where $x(\mathrm{Cu}) - x(\mathrm{In}) = 0$, superimposed with experimental data obtained by Wierzbinska-Miernik.[106] From this figure it can be seen that the proposed thermodynamic description reproduces enthalpy of mixing well. Similarly, Fig. 30 shows very good agreement between calculated and measured activity of In in liquid Ag-Cu-In at 1173 K for an intersection $x(\mathrm{Ag}) - x(\mathrm{Cu}) = 0$ by Wierzbinska-Miernik.[106] Figures 31 and 32 show

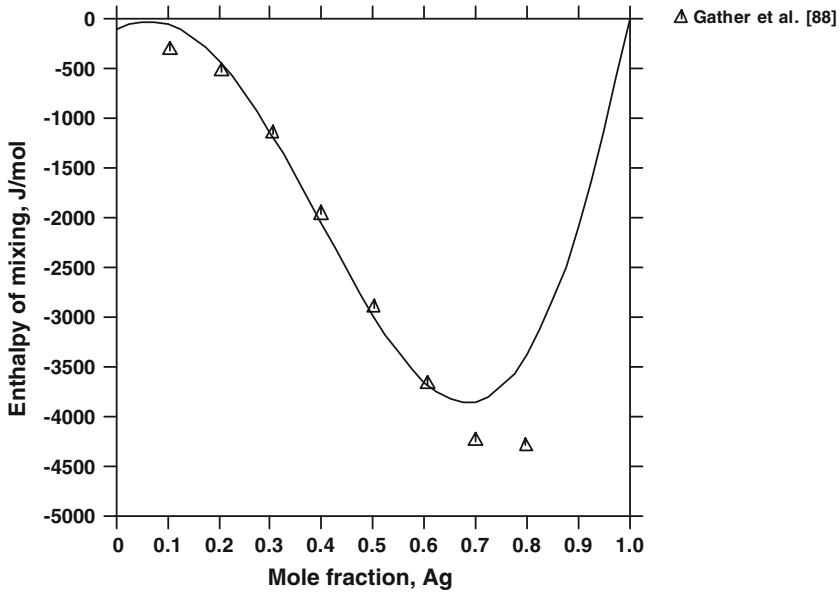

Fig. 31. Enthalpy of mixing of liquid Ag-In-Sn for intersection $4 \times x(\mathrm{Sn}) - x(\mathrm{In}) = 0$ at 1253 K superimposed with data obtained by Gather et al.[87]

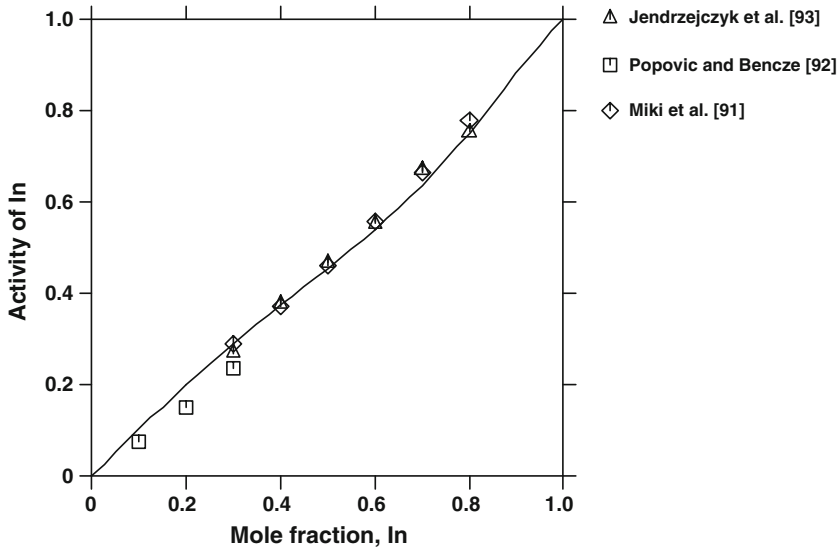

Fig. 32. Activity of indium in ternary Ag-In-Sn for intersection $x(\mathrm{Ag}) - x(\mathrm{Sn}) = 0$ at 1273 K superimposed with experimental data.

the calculated enthalpy of mixing and activity of In in the ternary Ag-In-Sn system, respectively. The enthalpy of mixing was calculated for intersection $4 \times x(\mathrm{Sn}) - x(\mathrm{In}) = 0$ at 1253 K and superimposed with experimental data obtained by Gather et al.[85] Activity of indium was calculated at 1273 K for an intersection $x(\mathrm{Ag}) - x(\mathrm{Sn}) = 0$. From both figures it can be seen that the calculation reproduced experimental data well. Figure 33 shows the calculated mixing enthalpy of liquid Ag-Cu-Sn at 1173 K for an intersection $x(\mathrm{Ag}) - x(\mathrm{Cu}) = 0$, together with experimental data obtained by Luef et al.[95] The calculation agrees well with experimental data for high concentration of tin; however, for concentration of Sn smaller than 0.5 mol fraction, the experimental data exhibits less negative heat effect than calculated function. Figure 34 shows calculated activity of Sn for an intersection $x(\mathrm{Ag}) - x(\mathrm{Cu}) = 0$ at 1300 K. The calculation agrees with experi-

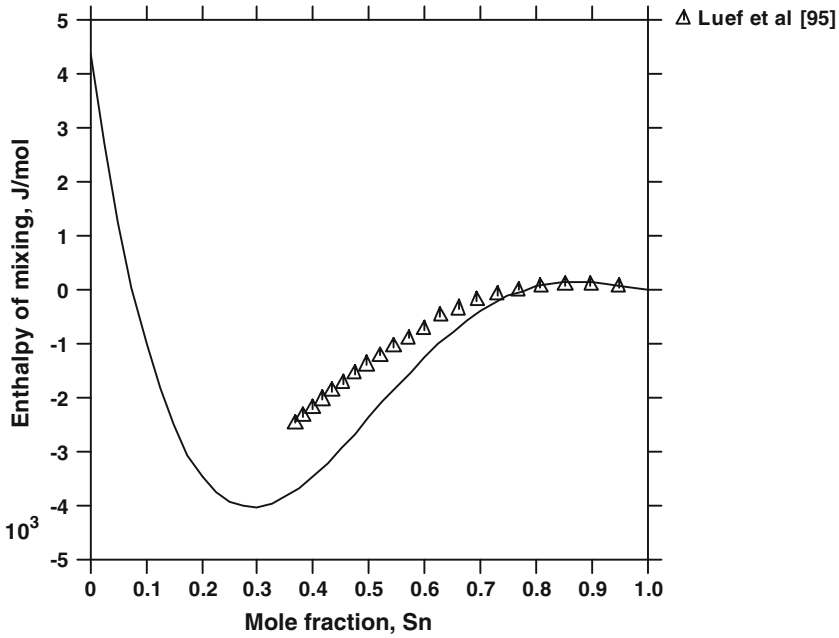

Fig. 33. Enthalpy of mixing of liquid Ag-Cu-Sn at 1173 K for intersection x(Ag) - x(Cu) = 0 together with experimental data.

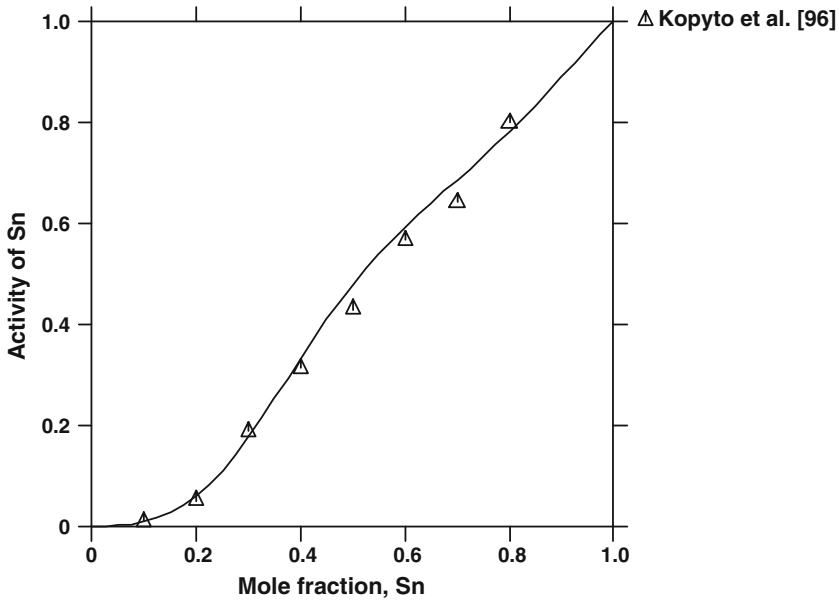

Fig. 34. Activity of Sn in liquid Ag-Cu-Sn for intersection x(Ag) - x(Cu) = 0 at 1300 K compared with experimental data.

mental data given by Kopyto et al.[95] Figures 35 and 36 display enthalpy of mixing of liquid Cu-In-Sn and activity of In in this system, respectively. The enthalpy of mixing was calculated for an intersection x(Cu) - x(In) = 0 at 1173 K, and the calculated function shows agreement with experimental data obtained by Li et al.[113] The activity of In in liquid Cu-In-Sn for intersection x(Cu) - x(Sn) = 0 at 1173 K reproduced the experimental data given by Jendrzejczyk-Handzlik et al.[112] well.

Besides a comparison of the calculated phase equilibria and thermodynamic properties with experimental data, the solidification path of promising lead-free solder was compared with differential thermal analysis (DTA) results as well as with literature information.[117] The quaternary alloy Sn-1.5Ag-0.7Cu-9.5In (wt.%) was chosen to check by

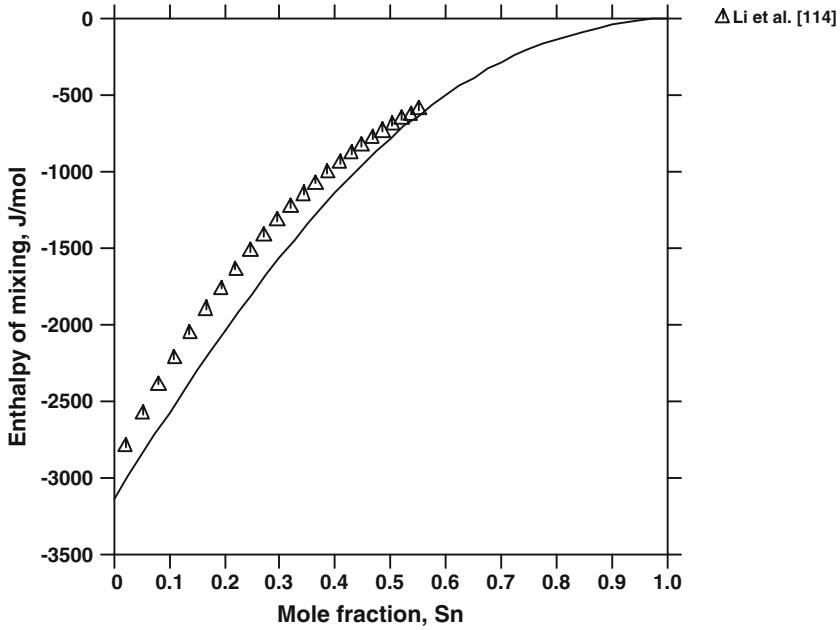

Fig. 35. Enthalpy of mixing of liquid Cu-In-Sn at 1173 K for intersection x(Cu) - x(In) = 0 together with experimental data.

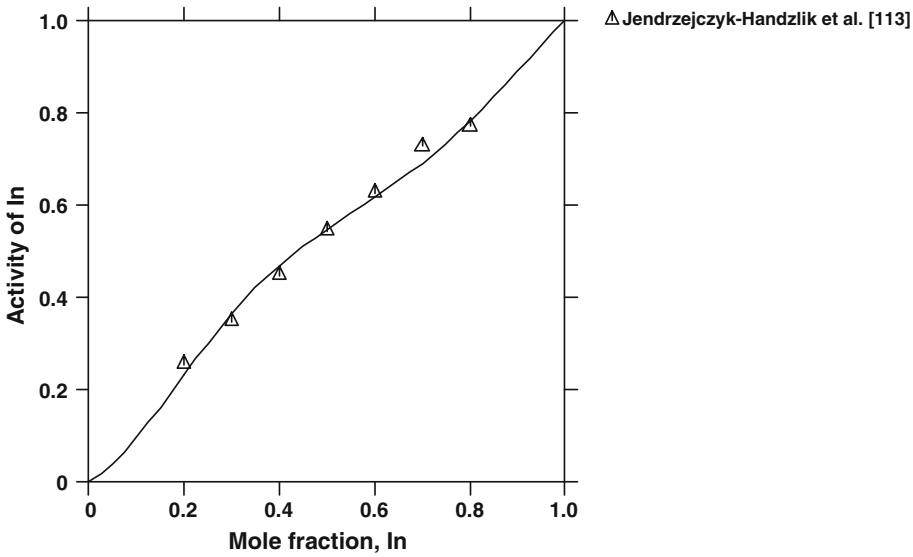

Fig. 36. Activity of In in liquid Cu-In-Sn for intersection x(Cu) - x(Sn) = 0 at 1173 K superimposed with experimental data.

DTA experiment. It is worth adding here that the same sample composition was used in Sopousek et al.'s[117] work. The calculated solidification path using the Scheil model is shown in Fig. 37, and temperatures of the reactions are given in Table III. Figures 38 and 39 show the heating curve with heating rate 5°/min. Based on Figs. 37–39 and comparison with experimental data, one can say that the proposed thermodynamic description of the quaternary Ag-Cu-In-Sn system reproduces well the solidification process of promising lead-free solder Sn-1.5Ag-0.7Cu-9.5In (wt.%). Figure 40 shows calculated isothermal section of the quaternary alloy at 623 K for constant concentration of Sn equal to 0.883 weight fraction. It should be mentioned here that Fig. 40 is not a phase diagram but a projection, because the tie-lines do not lie in the plane of the figure.

Table III. Calculated solidification path of the alloy Sn-1.5Ag-0.7Cu-9.5In (wt.%)

T (°C)	Reaction
208.68	LIQUID → INSN4
207.58	LIQUID → INSN4
207.51	LIQUID → INSN4 + ETA
199.61	LIQUID → INSN4 + ETA
198.49	LIQUID → INSN4 + ETA + HCP_A3
188.79	LIQUID → INSN4 + ETA + HCP_A3
188.72	LIQUID + ETA + HCP_A3 → INSN4 + CUIN_GAMMA
188.62	LIQUID → INSN4 + ETA + CUIN_GAMMA
154.82	LIQUID → INSN4 + ETA + CUIN_GAMMA
154.74	LIQUID + ETA + CUIN_GAMMA → INSN4 + ETA
154.44	LIQUID → INSN4 + ETA
130.64	LIQUID → INSN4 + ETA
129.4	LIQUID → INSN4 + ETA + CUIN_GAMMA
115.1	LIQUID → INSN4 + ETA + CUIN_GAMMA
114.33	LIQUID → INSN4 + ETA + CUIN_GAMMA + IN3SN
114.33	INSN4 + ETA + CUIN_GAMMA + IN3SN

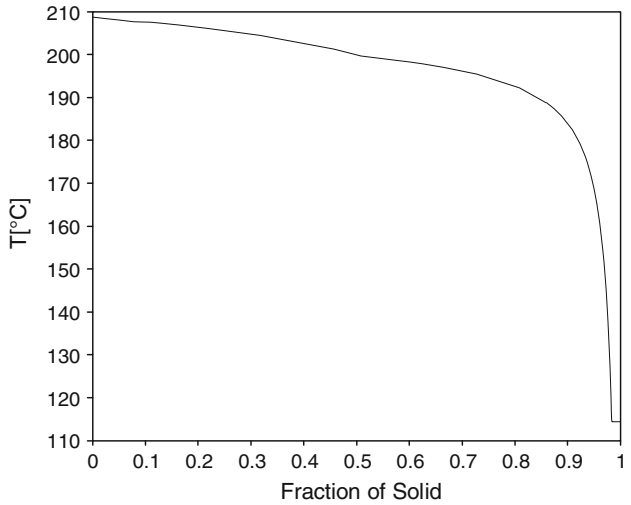

Fig. 37. Calculated solidification path of the alloy Sn-1.5Ag-0.7Cu-9.5In (wt.%).

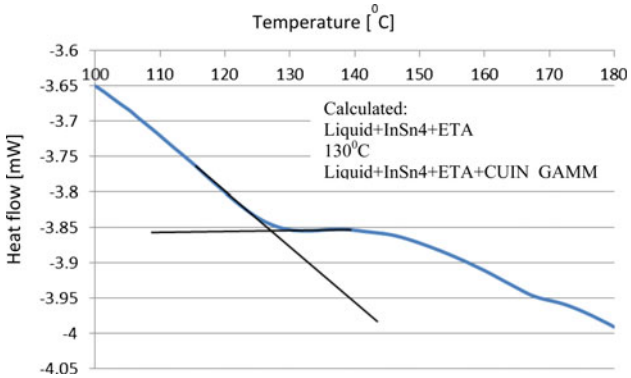

Fig. 38. DTA result, part I: composition of the sample Sn-1.5Ag-0.7Cu-9.5In (wt.%).

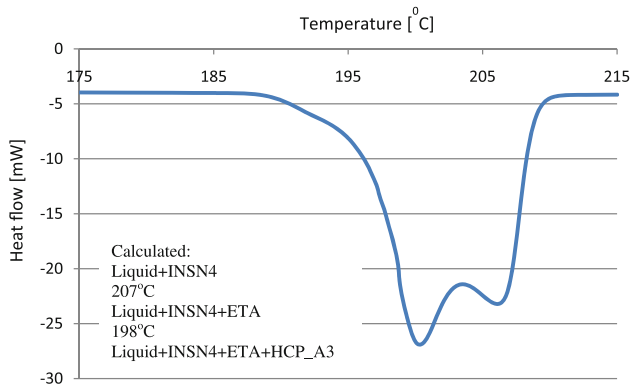

Fig. 39. DTA result, part II: composition of the sample Sn-1.5Ag-0.7Cu-9.5In (wt.%).

CONCLUSIONS

A new thermodynamic description of the quaternary Ag-Cu-In-Sn system is proposed. The Gibbs energies obtained in this work describe the thermodynamic properties of the phases as well as the phase equilibrium well. Inconsistent descriptions of CUIN_GAMMA in the ternary Ag-Cu-In system were found in the literature, suggesting that experimental investigation into this ternary system is warranted. DTA experiments performed on the promising lead-free solder Sn-1.5Ag-0.7Cu-9.5In (wt.%) agreed well with the calculated solidification path. The obtained thermodynamic database can provide a basis for future calculations of atomic mobilities in this quaternary system.

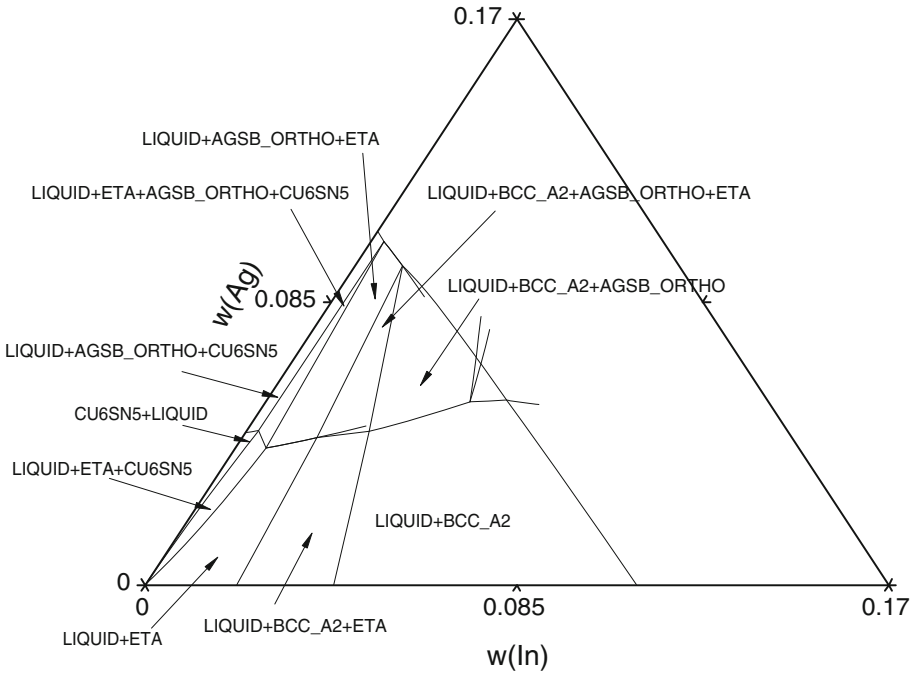

Fig. 40. Calculated isothermal section of the quaternary alloy at 623 K for constant concentration of Sn equal to 0.883 weight fraction.

ACKNOWLEDGEMENTS

This work was supported by the Taiwan National Science Council under Grant 99-2218-E-155-005. The author is grateful to Mr. Kai-Chien Zhang for performing the DTA experiment.

REFERENCES

1. J.H. Lee, C.W. Lee, and J.H. Kim, *Quaternary Pb-free Solder Composition Incorporating Sn-Ag-Cu-In* (Patentdocs 2008), http://www.faqs.org/patents/app/20080292493. Accessed 10 January 2011.
2. L. Kaufman and H. Bernstein, *Computer Calculations of Phase Diagrams* (New York: Academic, 1970).
3. F.H. Hayes, H.L. Lukas, G. Effenberg, and G. Petzow, *Z. Metallkde.* 77, 749 (1986).
4. O.J. Kleppa, *Acta Metall.* 3, 255 (1955).
5. R. Castanet, Y. Claire, and M. Laffitte, *J. Chim. Phys.* 67, 789 (1970).
6. T. Nozaki, M. Shimoji, and K. Niwa, *Trans. JIM* 7, 52 (1966).
7. R. Beja, *C. R. Acad. Sci.* 267C, 123 (1968).
8. C.B. Alcock, *Acta Metall.* 21, 1003 (1973).
9. G. Qi, *Mater. Trans. JIM* 30, 75 (1989).
10. D. Jendrzejczyk and K. Fitzner, *Thermochim. Acta* 433, 61 (2005).
11. T. Nozaki, *Mater. Trans. JIM* 7, 52 (1966).
12. O.J. Kleppa, *J. Phys. Chem.* 60, 846 (1956).
13. D.B. Masson, *Metall. Trans. A* 4A, 991 (1973).
14. Z. Moser, W. Gasior, J. Pstrus, W. Zakulski, I. Ohnuma, X.J. Liu, Y. Inohana, and K. Ishida, *J. Electron. Mater.* 30, 1120 (2001).
15. F. Weibke, *A. Anorg. Chem.* 222, 145 (1935).
16. A.N. Campbell, *Can. J. Chem.* 48, 1703 (1970).
17. W. Hume-Rothery, *Phil. Trans. R. Soc. Lond. Ser. A* 233, 1 (1936).
18. E.A. Owen, *Phil. Mag.* 27, 294 (1939).
19. M.E. Staumanis, *Trans. Metall. Soc. Lond. AIME* 233, 964 (1965).
20. F. Witting and E. Gehring, *Z. Naturforsch.* A18, 351 (1963).
21. G. Laurie, A. Morrison, and J. Pratt, *Trans. AIME* 236, 1390 (1966).
22. K. Itagaki and A. Yazawa, *J. Jpn. Inst. Met.* 32, 1294 (1968).
23. R. Castanet, Y. Claire, and M. Laffitte, *J. Phys. Chem.* 66, 1276 (1969).
24. R. Rakotomavo, M. Guane-Escard, J.P. Bros, and P. Guane, *Ber. Bunsen-Ges. Phys. Chem.* 88, 663 (1984).
25. T. Nozaki, M. Shimoji, and K. Niwa, *Ber. Bunsen-Ges. Phys. Chem.* 70, 207 (1966).
26. K. Okajima and H. Sako, *Mater. Trans. JIM* 15, 51 (1974).
27. R.O. Frantik and H.J. McDonald, *Trans. Electrochem. Soc.* 88, 253 (1945).
28. J.A. Yanko, A.E. Drake, and F. Hovorka, *Trans. Electron. Soc.* 89, 357 (1964).
29. G.R.B. Elliot and J.F. Lemons, *J. Electron. Soc.* 114, 935 (1967).
30. P.J.R. Chowdhury and A. Gosh, *Metall. Trans.* 2, 2171 (1971).
31. P. Kubashewski and C.B. Alcock, *J. Chem. Thermodyn.* 4, 171 (1972).
32. R. Fahri, G. Petot-Ervas, and C. Petot, *Phys. Chem. Liq.* 5, 171 (1974).
33. S. Seetharaman and L.I. Staffansson, *Chem. Scripta* 10, 61 (1976).
34. M. Iwase, M. Yasuda, S. Miki, and T. Mori, *Trans. JIM* 19, 654 (1978).
35. K. Kameda, Y. Yoshida, and S. Sakairi, *J. Jpn. Inst. Met.* 44, 858 (1980).
36. T. Yamayi and E. Kato, *Metall. Trans.* 3, 1002 (1972).
37. P.C. Wallbrecht, R. Blachnik, and K.C. Mills, *Thermochim. Acta* 46, 167 (1981).
38. C.T. Heycock and F.H. Neville, *Phil. Trans. R. Soc. Lond. Ser. A* 189, 25 (1897).
39. A.J. Murphy, *J. Inst. Chem.* 35, 107 (1926).
40. G.J. Petrenko, *Z. Anorg. Chem.* 53, 200 (1907).
41. W. Hume-Rothery and P.W. Reynolds, *Proc. R. Soc. Lond. Ser. A* 160, 282 (1937).
42. M.M. Umansky, *Z. Fiz. Khim.* 14, 846 (1940).
43. O.J. KLeppa, *J. Phys. Chem.* 60, 852 (1956).
44. R. Beja (Ph.D. thesis, Marsseile, 1969).

45. T. Azakami and A. Yazawa, *J. Min. Metall. Inst. Jpn.* 85, 97 (1969).
46. K. Itagaki and K. Yazawa, *J. Jpn. Inst. Met.* 35, 383 (1971).
47. T. Kang, H.V. Kehiaian, and R. Castanet, *J. Calorim. Anal. Therm.* 7, 371 (1976).
48. T. Kang, H.V. Kehiaian, and R. Castanet, *J. Less-Common Met.* 53, 153 (1977).
49. K.P. Jagannathan and A. Gosh, *Trans. Ind. Inst. Met.* 27, 298 (1974).
50. K.T. Jacob and C.B. Alcock, *Acta Metall.* 21, 1011 (1973).
51. F. Weibke and H. Eggers, *Z. Anorg. Allg. Chem.* 220, 273 (1934).
52. W. Hume-Rothery, G.V. Raynor, and H.K. Packer, *J. Inst. Met.* 66, 209 (1940).
53. J. Reynolds, W.A. Wissman, and W. Hume-Rothery, *J. Inst. Met*. 80, 637 (1951–52).
54. K.C. Jain, M. Ellner, and K. Schubert, *Z. Metallkd.* 63, 456 (1972).
55. E.A. Owen and D.P. Morris, *J. Inst. Met.* 73, 471 (1974).
56. R.O. Jones and E.A. Owen, *J. Inst. Met*. 82, 479 (1953–54).
57. M.E. Straumanis and L.S. Yu, *Acta Crystallogr. A* 25, 676 (1969).
58. P.C. Walbrecht, R. Blachnik, and K.C. Mills, *Thermochim. Acta* 48, 69 (1981).
59. A.S. Koster, L.R. WolfG, and J. Visser, *Acta Crystallogr. B* 36, 3094 (1980).
60. J.W.G.A. Vroljik and L.R. Wolf, *J. Cryst. Growth.* 48, 85 (1980).
61. O.J. Kleppa, *J. Phys. Chem.* 60, 852 (1956).
62. R. Hultgren, P.D. Desai, D.T. Hawkins, M. Gleiser, and K. Kelly, *Selected Values of the Thermodynamic Properties of Binary Alloys* (Material Park, Ohio: American Society for Metals, 1973).
63. S. Takeuci, O. Uemura, and S. Ikeda, *Sci. Rep. Tohoku Imp. Univ.* 25A, 41 (1974).
64. A. Yazawa and K. Itagaki, *Trans. JIM* 16, 679 (1975).
65. Y. Iguchi, H. Shimoji, S. Ban-Ya, and T. Fuwa, *Tetsu-to-Hagané* 63, 349 (1977).
66. M.J. Pool, B. Predel, and E. Schultheiss, *Thermochim. Acta* 28, 349 (1979).
67. J.J. Lee, B.J. Kim, and W.S. Min, *J. Alloy. Compd.* 202, 237 (1993).
68. C.B. Alcock, R. Sridhar, and R.C. Svedberg, *Acta Metall.* 17, 839 (1969).
69. J.P. Hager, S.M. Howard, and J.H. Jones, *Metall. Trans.* 1, 415 (1970).
70. K. Ono, S. Nishi, and T. Oishi, *Trans. JIM* 25, 810 (1984).
71. T. Oshi, T. Hiruma, and J. Moriyama, *J. Jpn. Inst. Met.* 36, 481 (1972).
72. A.K. Sengupta, K.P. Jagganathan, and A. Gosi, *Metall Trans.* 9B, 141 (1978).
73. C.B. Alcock and K.T. Jacob, *Acta Metall.* 22, 539 (1974).
74. F. Sommer, W. Balbach, and B. Predel, *Thermochim. Acta* 33, 119 (1979).
75. B. Predel and U. Schallner, *Mater. Sci. Eng.* 10, 249 (1972).
76. M. Hamasumi and N. Takamoto, *Nippon Kinzoku Gakkaishi* 1, 251 (1937).
77. M. Hamasumi, *Nippon Kinzoku Gakkaishi* 2, 147 (1938).
78. C.T. Heycock and F.H. Neville, *Phil. Trans. Roy. Soc*. 189A, 47, 62 (1897).
79. O. Bauer and O. Vollenbruck, *Z. Metallkd*. 15, 119, 191 (1923).
80. D. Stockdale, *J. Inst. Met.* 34, 111 (1925).
81. A.R. Raper, *J. Inst. Met.* 38, 217 (1927).
82. J. Vero, *Z. Anorg. Chem.* 218, 402 (1934).
83. C. Haase and F. Pawlek, *Z. Metallkde.* 28, 73 (1936).
84. B.D. Bastow and D.H. Kirwood, *J. Inst. Met.* 99, 277 (1971).
85. B.-J. Lee, C.-S. Oh, and J.-H. Shim, *J. Electron. Mater.* 25, 983 (1996).
86. N. Moelans, K.C. Hari Kumar, and P. Wollants, *J. Alloy. Compd.* 360, 98 (2003).
87. B. Gather, P. Schröter, and R. Blachnik, *Z. Metallkde.* 78, 280 (1987).
88. M. Alaoui-Elbelghiti (Ph.D. Thesis, Rabat, Morocco, 1998).
89. C. Luef, H. Flandorfer, and H. Ipser, *Metall. Mater. Trans. A* 36, 1273 (2005).
90. T. Miki, N. Ogawa, T. Nagasaka, and M. Hino, *Mater. Trans.* 42, 732 (2001).
91. L. Bencze and A. Popovic, *Int. J. Mass. Spectrom.* 270, 139 (2008).
92. D. Jendrzejczyk, W. Gierlotka, and K. Fitzner, *J. Chem. Therm.* 41, 250 (2009).
93. Z.J. Liu, Y. Inohana, Y. Takaku, I. Ohnuma, R. Kainuma, K. Ishida, Z. Moser, W. Gasior, and J. Pstrus, *J. Electron. Mater.* 31, 1139 (2002).
94. C. Luef, H. Flandorfer, and H. Ipser, *Z. Metallkd.* 93, 151 (2004).
95. M. Kopyto, B. Onderka, and L.A. Zabdyr, *Mater. Chem. Phys.* 122, 480 (2010).
96. E. Gebhardt and G. Petzow, *Z. Metallkde.* 50, 597 (1959).
97. S.S. Shen (Ph.D. Thesis, University of Denver, 1969).
98. S.S. Shen, P.J. Spencer, and M.J. Pool, *Trans. AIME* 245, 603 (1969).
99. V.N. Fedotov, O.E. Osinchev, and E.T. Yushkina, *Fazovye Ravnovesiya Met. Splavakh*, ed. N.V. Ageev and L.A. Petrova (1981), p. 42.
100. V.N. Fedotov, O.E. Osinchev, and E.T. Yushkina, *Phase Diagrams of Metallic Systems*, Vol. 26, ed. N.V. Ageev and L.A. Petrova (1982), p. 149.
101. C.M. Miller, I.E. Anderson, and J.K. Smith, *J. Electron. Mater.* 23, 595 (1994).
102. S. Chada, W. Laub, R.A. Fournelle, and D. Shangguan, *J. Electron. Mater.* 26, 11 (1999).
103. K.W. Moon, W.J. Boettinger, U.R. Kattner, F.S. Biancaniello, and C.A. Handwerker, *J. Electron. Mater.* 29, 1122 (2000).
104. M.E. Loomans and M.E. Fine, *Metall. Mater. Trans. A* 31, 1152 (2000).
105. Y-w Yen and S-w Chen, *J. Mater. Res.* 19, 2298 (2004).
106. A. Wierzbicka-Miernik, *Inż. Materialowa* 28, 889 (2007).
107. E. Gebhardt and M. Dreher, *Z. Metallkd.* 42, 230 (1951).
108. E. Gebhardt and M. Dreher, *Z. Metallkd.* 43, 357 (1952).
109. C.G. Woychik and T.B. Massalski, *Metall. Trans.* A19, 13 (1988).
110. Z. Bahari, M. Elgadi, J. Rivat, and J. Dugue, *J. Alloy. Compd.* 477, 152 (2009).
111. K. Fitzner, *Arch. Met.* 29, 109 (1984).
112. D. Jendrzejczyk–Handzlik, W. Gierlotka, and K. Fitzner, *J. Chem. Thermodyn.* 41, 250 (2009).
113. A. Popovic and L. Bencze, *Int. J. Mass Spectrom.* 257, 41 (2006).
114. Z. Li, S. Knott, Z. Qiao, and A. Mikula, *Mater. Trans.* 47, 2025 (2006).
115. X.J. Liu, H.S. Liu, I. Ohnuma, R. Kainuma, K. Ishida, S. Itabashi, K. Kameda, and K. Yamaguchi, *J. Electron. Mater.* 30, 1093 (2001).
116. S.-k. Lin, T.-y. Chung, S.-w. Chen, and C.-h. Chang, *J. Mater. Res.* 24, 2628 (2009).
117. J. Sopousek, M. Palcut, E. Hudolova, and J. Janovec, *J. Electron. Mater.* 39, 312 (2010).
118. PURE 4.4 SGTE Pure Elements (Unary) Database, Scientific Group Thermodata Europe 1991–2006.
119. E.A. Guggenheim, *Mixtures* (Oxford: Clarendon, 1952).
120. L. Hans, B. Sundman, and F. Suzana, *Computational Thermodynamics: CALPHAD Method* (Cambridge: Cambridge University Press, 2007).
121. ThermoCalc v. S. Foundation Computational Thermodynamic, Stockholm, Sweden, 2008.
122. R. Schmid-Fetzer, D. Andersson, P.Y. Chevalier, L. Eleno, O. Fabrichnaya, U.R. Kattner, B. Sundman, C. Wang, A. Watson, L. Zabdyr, and M. Zinkevich, *Calphad* 31, 38 (2007).
123. Pandat, CompuTherm LLC, 437 S. Yellowstone Dr. Suite 217 Madison, WI 53719 USA.